NASA
CR
3598
c.1

LOAN COPY: RETURN TO AFWL
TECHNICAL LIBRARY, KIRTLAND

TECH LIBRARY KAFB, NM
0062133

NASA Contractor Report 3598

# Development and Test of a Microwave Ice Accretion Measurement Instrument (MIAMI)

Bertram Magenheim and James K. Rocks

CONTRACT NAS3-22765
NOVEMBER 1982

NASA

TECH LIBRARY KAFB, NM

0062133

NASA Contractor Report 3598

# Development and Test of a Microwave Ice Accretion Measurement Instrument (MIAMI)

Bertram Magenheim and James K. Rocks
*Ideal Research Inc.*
*Rockville, Maryland*

Prepared for
Lewis Research Center
under Contract NAS3-22765

National Aeronautics
and Space Administration

**Scientific and Technical**
**Information Branch**

1982

## SUMMARY

A Microwave Ice Accretion Measurement Instrument (MIAMI) incorporating a microprocessor has been developed that can

1. Detect the presence of ice and sound an alarm.
2. Measure and digitally display ice thickness.
3. Measure and digitally display ice accretion rate.
4. Plot ice thickness, accretion rate and other parameters on a pen recorder.
5. Log and print out a permanent record of ice thickness and ice accretion rate versus time.
6. Store data for future statistical analysis and printout.

Ice thickness indications to approximately 1/4 inch were frequently observed; however, it is believed that calibration techniques were good only up to 1/8 inch. Theory, verified during this program, indicates that larger ice thickness measurements are possible by resorting to larger transducers and lower operating frequencies. Ice thickness to 1 inch is not considered unreasonable.

The instrument is non-intrusive, that is, it does not use probes; but is mounted under the surface being monitored and does not interfere with its aerodynamic properties.

One or more transducers may be mounted anywhere on an airfoil or other aircraft surfaces - all can be monitored by a single microprocessor.

Electro-thermal deicing of the MIAMI to remove existing ice is feasible. Ice removal is not necessary, however, until the ice thickness exceeds the dynamic range of the instrument.

The MIAMI transducer is constructed from solid state components all of which have very little mass and are therefore capable of

being miniaturized and ruggedized. The unminiaturized experimental model was only 7" x 4" x 1 ½" in size.

The development described herein represents research that was performed over a period of one year at IDEAL RESEARCH INC. The fundamental principle exploited is that layers of ice accreting on the surface of a resonant surface waveguide will alter its resonant frequency. The degree of shift of the resonance is related to thickness of the ice layers. To take advantage of this phenomenon the research proceeded in two areas: (1) the microwave transducer and (2) the microprocessor for monitoring resonant frequency and displaying ice thickness and accretion rate.

The phenomenon observed and utilized are the result of the molecular and dielectric properties of water and ice. The work thus represents, for the first time, research into one of the basic physical phenomenon underlying the formation and adhesion of ice to aircraft surfaces.

TABLE OF CONTENTS


| | | Page |
|---|---|---|
| | SUMMARY | iii |
| 1.0 | INTRODUCTION | 1 |
| 2.0 | RESULTS OF EXPERIMENTAL PROGRAM | 2 |
| | 2.1 Description of the MIAMI | 2 |
| | 2.2 Performance of the MIAMI | 8 |
| | 2.3 Measured Dynamic Range of the MIAMI-Model No. 6 | 16 |
| | 2.4 Effects of Liquid Water on the MIAMI at Temperatures Above Freezing | 18 |
| 3.0 | MIAMI DESIGN THEORY | 19 |
| | 3.1 Choosing MIAMI Dimensions | 23 |
| | 3.2 Construction and Test of Experimental Surface Waveguides | 26 |
| | 3.3 Agreement Between Theory and Experiment Measured Tuning Curves | 32 |
| | 3.4 Coupling to the Surface Waveguide | 34 |
| 4.0 | THE MIAMI SYSTEM THEORY | 35 |
| | 4.1 Theoretically Derived Relation Between Ice Thickness and Frequency Index | 37 |
| | 4.2 Variation of Dynamic Range with MIAMI Dimensions | 40 |
| 5.0 | RECOMMENDATIONS | 43 |
| 6.0 | LIST OF SYMBOLS | 45 |

APPENDIX 1

1.0 TRANSFER CHARACTERISTICS OF DAC AND THE VTO DRIVER. . . . . 47

2.0 TRANSFER CHARACTERISTICS OF VTO 8580 MEASURED . . . 48

3.0 FREQUENCY TRANSFER CHARACTERISTICS OF VTO (DERIVATION). . . . . 49

4.0 MEASURED CHANGE IN FREQUENCY (df) WITH CHANGE IN FREQUENCY INDEX (di). . . . . 54

5.0 EQUIVALENT CIRCUIT THEORY OF MIAMI TRANSDUCER . . . 57

APPENDIX 2 - SYSTEM DOCUMENTATION

1.0 THE MICROPROCESSOR. . . . . 59

1.1 Peak Following Algorithm . . . . . 63

1.2 Averaging Subroutine . . . . . 64

2.0 THE COMPUTER PROGRAM. . . . . 65

2.1 Flow Charts. . . . . 65

2.2 Main Control Program, Definitions. . . . . 69

2.3 Program Listing. . . . . 71

3.0 COMPUTER HARDWARE . . . . . 73

4.0 MIAMI OPERATING INSTRUCTIONS. . . . . 77

# DEVELOPMENT AND TEST OF A MICROWAVE ICE ACCRETION MEASUREMENT INSTRUMENT (MIAMI).

## 1.0 INTRODUCTION

The purpose of this program was to perform an engineering study to confirm that it is technically and economically feasible to develop a microwave instrument system (MIAMI) for research purposes that can simultaneously perform the following functions.

a. Detect the presence of ice.

b. Measure ice thickness.

c. Measure ice accretion rate.

"Icing instrumentation (Reference 1) is an area of research that is so fundamental that it is probably the most important area." There can not be an "icing science," without the ability to measure the icing environment accurately. In the 1940's and 1950's, relatively clumsy and slow measurement techniques were used with questionable accuracy. Advances in instrumentation have been so dramatic since that time that it is now possible to achieve measurements of icing parameters with real time data displays. The "Microwave Ice Accretion Measurement Instrument" (MIAMI) developed during this program is one such device that can be used as a research, as well as an operational, instrument.

1. Milton A. Beheim "Executive Summary of Aircraft Icing Specialists Workshop" NASA Conference Publication 2086 **(FAA-RD-78-109)** Aircraft Icing, July 19-21, 1978, **Page 8.**

## 2.0 RESULTS OF EXPERIMENTAL PROGRAM

### 2.1 Description of the MIAMI

The MIAMI developed in this program is a device that is responsive to the thickness of ice accreting on its surface. An illustration of the MIAMI transducer mounted on an airfoil is shown in Figure 1. Its real time output, illustrating the growth of ice on an airfoil mounted in the icing research tunnel (IRT), is shown in Figure 2. A photo of the MIAMI experimental model is shown in Figure 3. It consists of two major elements, a transducer for mounting under the surface being monitored and a microprocessor connected to the transducer by a long multiconductor cable. The microprocessor sends signals to the transducer and based upon the response received from the transducer computes the ice thickness and accretion rate which are digitally displayed on the front panel. The displays are instantaneous. The MIAMI can be programmed to log and printout a permanent record of ice thickness and accretion rate as a function of time. A sample printout appears as Figure 4. It can also be programmed to store ice thickness and accretion rate in computer memory for later statistical analysis for use in icing cloud studies.

Additional important features of the MIAMI transducer are that it is non-intrusive; it does not use probes protruding into the air stream but is flush mounted, with the surface being monitored. The MIAMI is constructed from components that can be packaged as miniature integrated circuits having almost negligible mass, enabling it to be mounted almost anywhere on the skin of the aircraft including rotor blades and engine inlets.

The transducer mounted just below the surface being monitored is a resonant microwave device, the resonant frequency of which is very sensitive to the thickness of ice accreting on its surface. As the ice layer grows, the resonant frequency is reduced as illustrated in Figure 5 a and b.

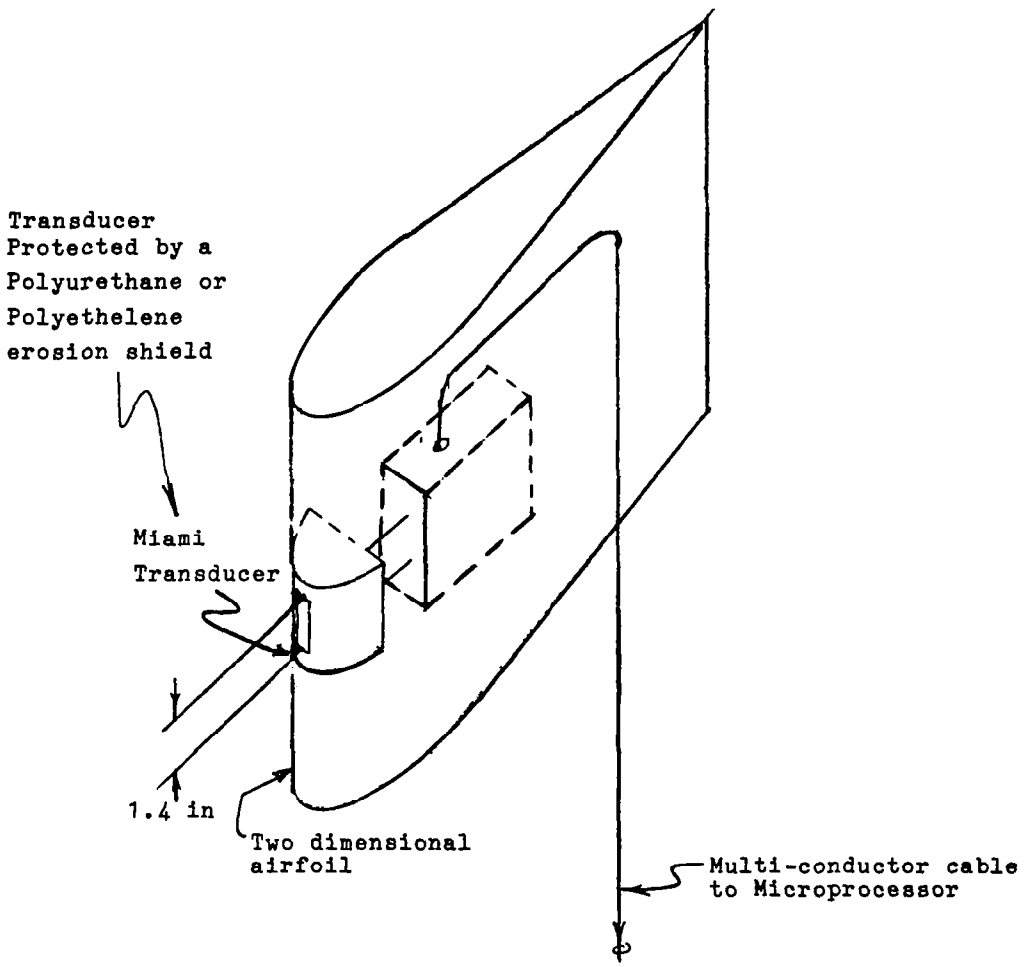


FIGURE 1 - MIAMI MOUNTED ON A TWO-DIMENSIONAL AIRFOIL

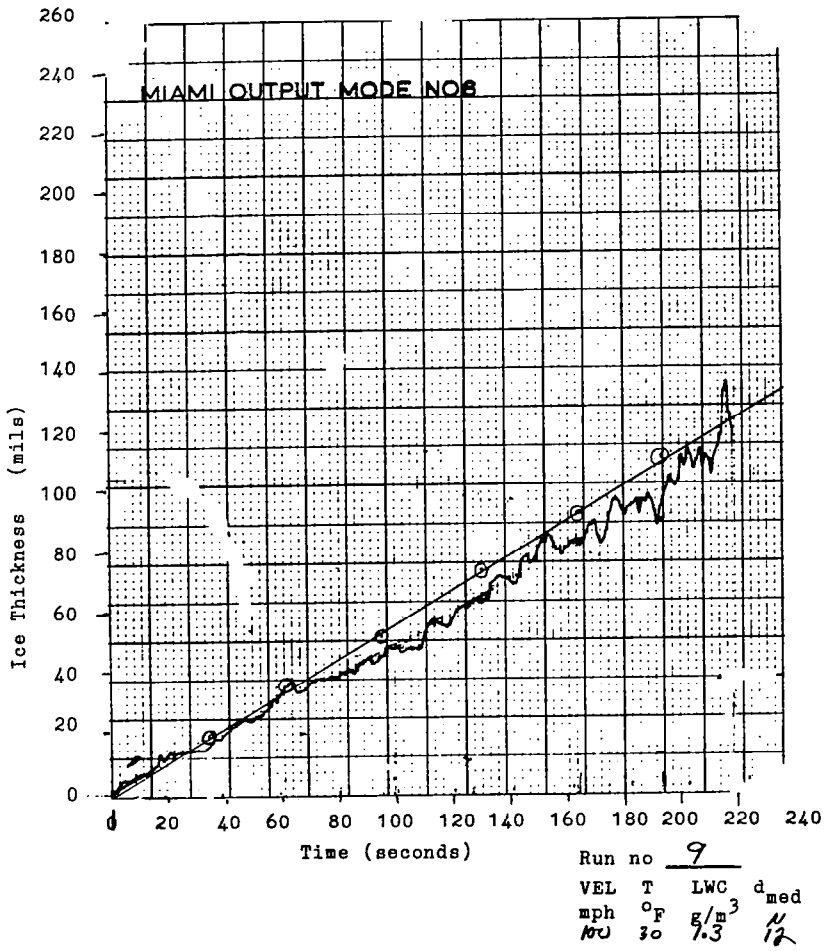


FIGURE 2 - TYPICAL PEN RECORDING OF MIAMI OUTPUT ILLUSTRATING ICE GROWTH IN REAL TIME

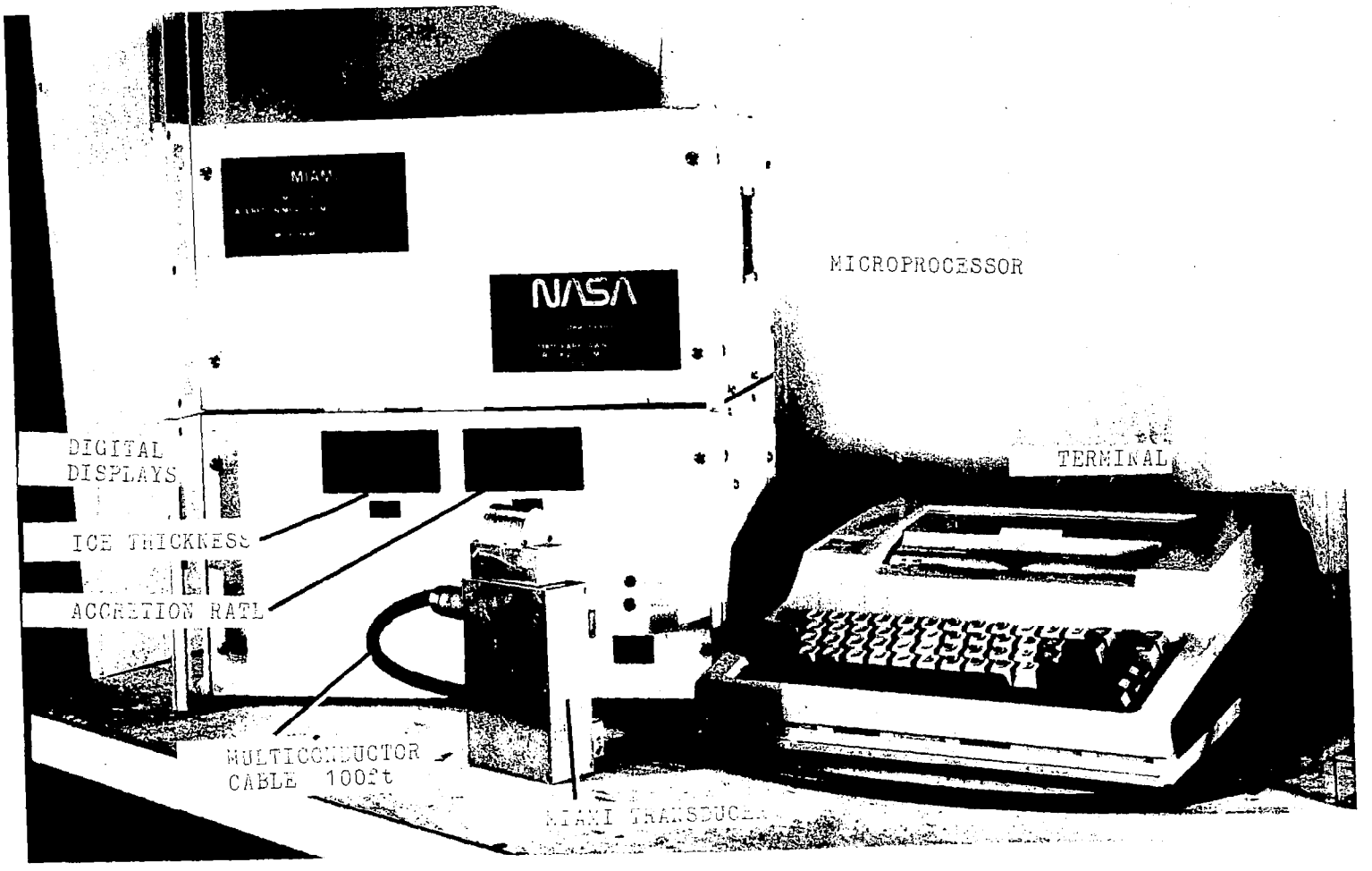


FIGURE 3- MIAMI EXPERIMENTAL MODEL

.....8/25/81 RUN NUMBER: 9
TUNNEL PRAMS: VEL=100 TEMP(F)=30 DROPLET SIZE=12 WATER CONTENT=1.3
COMMENTS:
TRANSIT COEFFICIENT: .93

| TIME | D-INDEX | TRANSIT ICE | MIAMI ICE |
|---|---|---|---|
| 34.80 | 367.00 | 18.60 | 14.59 |
| 61.20 | 646.00 | 37.20 | 35.29 |
| 94.76 | 759.00 | 55.80 | 45.99 |
| 127.36 | 937.00 | 74.40 | 65.27 |
| 163.16 | 1049.00 | 93.00 | 79.88 |
| 190.92 | 1165.00 | 111.60 | 99.07 |
| 0.00 | 0.00 | 0.00 | 0.00 |

.....8/25/81 RUN NUMBER: 10
TUNNEL PRAMS: VEL=100 TEMP(F)=30 DROPLET SIZE=15 WATER CONTENT=1.8
COMMENTS:
TRANSIT COEFFICIENT: .93

| TIME | D-INDEX | TRANSIT ICE | MIAMI ICE |
|---|---|---|---|
| 77.64 | 512.00 | 18.60 | 24.17 |
| 117.24 | 736.00 | 37.20 | 43.72 |
| 154.00 | 865.00 | 55.80 | 57.05 |
| 187.64 | 1016.00 | 74.40 | 75.27 |
| 216.20 | 0.00 | 0.00 | 0.00 |
| 0.00 | | | |

.....8/25/81 RUN NUMBER: 11
TUNNEL PRAMS: VEL=100 TEMP(F)=30 DROPLET SIZE=19 WATER CONTENT=2.5
COMMENTS:
TRANSIT COEFFICIENT: .93

| TIME | D-INDEX | TRANSIT ICE | MIAMI ICE |
|---|---|---|---|
| 36.92 | 332.00 | 18.60 | 12.70 |
| 87.80 | 624.00 | 37.20 | 33.34 |
| 122.48 | 745.00 | 55.80 | 44.61 |
| 146.96 | 846.00 | 74.40 | 54.98 |
| 172.52 | 869.00 | 93.00 | 57.49 |
| 191.92 | 954.00 | 111.60 | 67.32 |
| 214.28 | 928.00 | 130.20 | 64.20 |
| 0.00 | 0.00 | 0.00 | 0.00 |

FIGURE 4 - SAMPLE PRINTOUT PROVIDED BY THE MIAMI ILLUSTRATING PERMANENT RECORD OF ICE GROWTH HISTORY

(a)

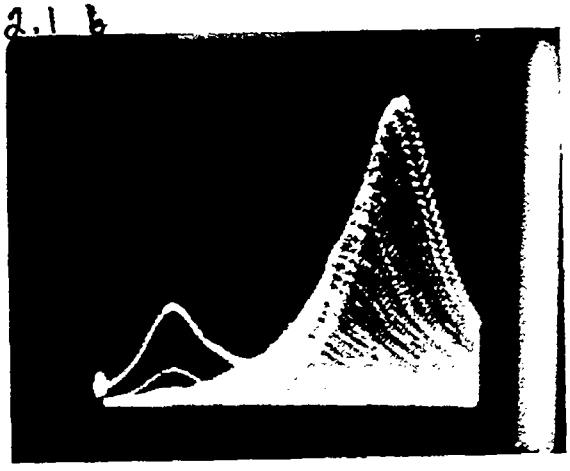

(b)

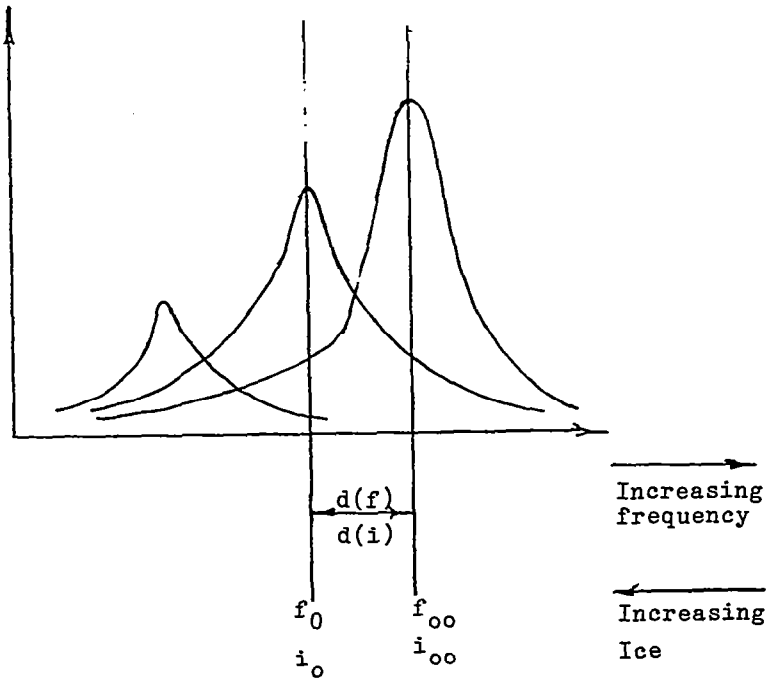


FIGURE 5 - VARIATION OF MIAMI RESONANCE AS ICE ACCRETES ON ITS SURFACE
(a) Storage oscilloscope trace
(b) Definition of symbols for use with oscilloscope trace

The microprocessor is programmed to continually monitor the change in resonant frequency (indicated by df in Figure 5) and convert this change into a dc voltage which is proportional to the ice thickness as illustrated in the real time recording shown in Figure 2.

## 2.2 Performance of the MIAMI

The MIAMI was tested in the icing research tunnel during two weeks in June and one week in August, 1981. Thirty-one tests were run in June and twenty-nine in August.

The purpose of the tests was to determine the ability of the MIAMI to measure the thickness of ice accreting on its surface under conditions simulating those of natural icing.

The transducer logic assumes that the ice is growing in uniform layers above it. This approximation is true if the transducer width w is small relative to major variations in the ice as illustrated in Figure 6a. When the ice is non-uniform, as illustrated in figure 6b, the reading produced by the MIAMI represents an average value of the ice thickness in the vicinity of the transducer.

For many every day aircraft applications the condition that the transducer be small relative to the gross variations in the ice layer is satisfied and the MIAMI readings of average thickness will closely represent the thickness of the ice layer. For research applications when the ice layers grow into odd shapes, care must be taken that the particular MIAMI chosen for the measurement is sufficiently smaller than the gross ice variations in its vicinity so that the readings are truly representative of the thickness of the ice accreting above it.

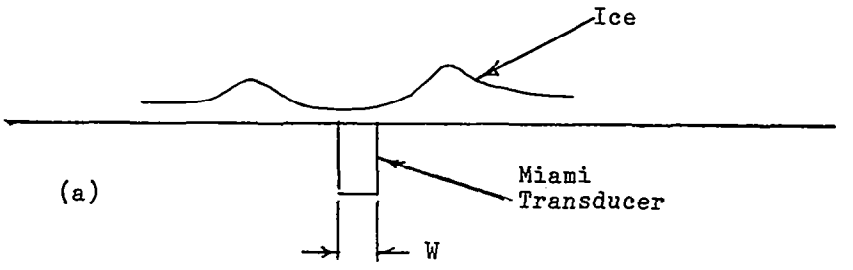


Transducer small relative to variations in ice

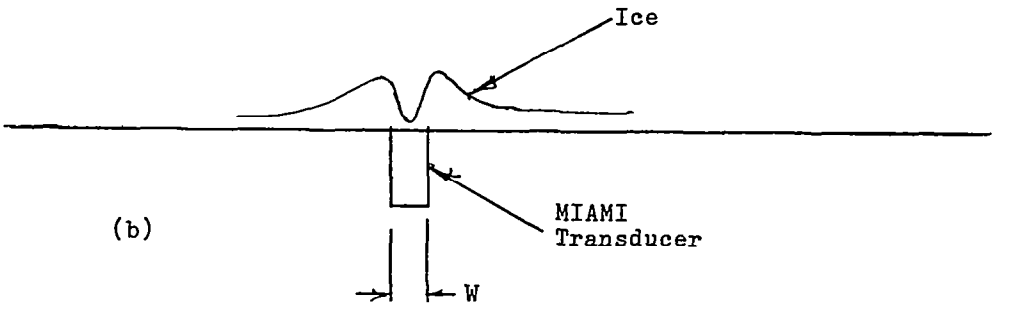


Transducer large relative to variations in ice.

FIGURE 6 - SIZE OF MIAMI TRANSDUCER RELATIVE TO GROSS VARIATIONS OF ICE THICKNESS

Impact ice under a wide range of tunnel conditions was permitted to accrete on the MIAMI transducer, which was mounted at the stagnation point of a two-dimensional airfoil, as shown in Figure 1, and the thickness of the ice was measured by the MIAMI and an independent means. The independent means used to measure ice thickness during this testing was a calibrated transit located in the control room viewing the ice layers accreting on the MIAMI surface. The accuracy of this technique, however, is limited to relatively thin layers of ice not more than about 125 mils.

Ice growth on the airfoil under certain cloud conditions was non-uniform, being less at the stagnation point than at neighboring locations. As the ice grew a time was reached when the transit could no longer see the ice at the stagnation point, it being obscured by the more rapid growth on either side of it. When this happened, the transit began to track the more rapidly growing ice, or horns, on either side of the stagnation point. This phenomena is illustrated in Figure 7 which is one of 18 plots demonstrating this phenomena. A more ideal way to test the MIAMI in thick ice would be to mount the MIAMI on a rotating cylinder since ice will accrete uniformly on this surface.

Examination of data taken in the icing research tunnel, overwhelmingly supports this thesis. The calibration of the MIAMI is thus based solely on data gathered during early growth stages when the ice is less than about 125 mils (1/8 in) thick and transit measurement and MIAMI measurements are in close agreement.

### 2.2.1 Calibration of the MIAMI

Equation 1 represents the theoretically derived relationship between ice thickness and shift in resonant frequency as derived in Section 3.0.

$$I = 1/k \ln (1-df/df_a) \qquad (1)$$

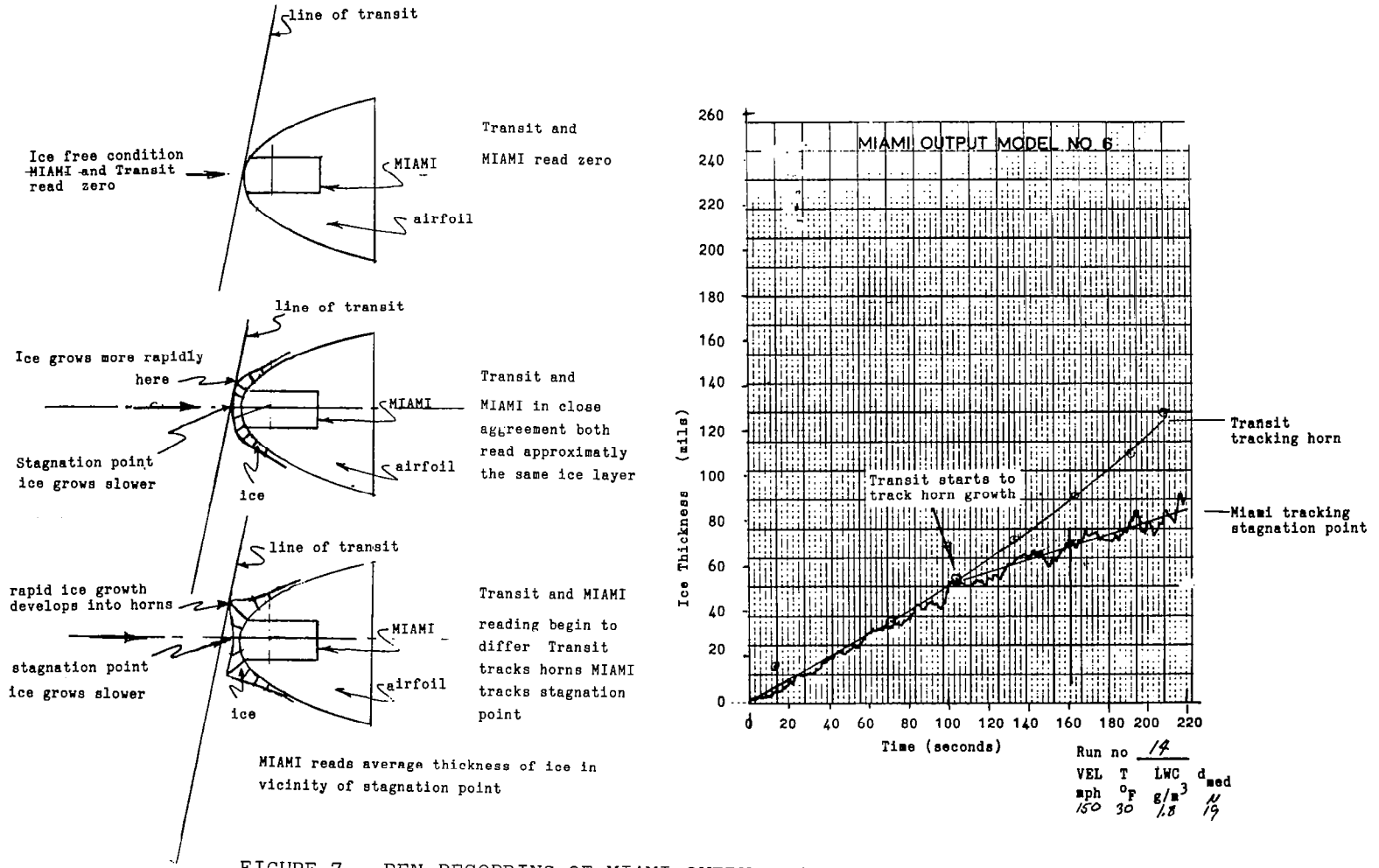


FIGURE 7 - PEN RECORDING OF MIAMI OUTPUT- ILLUSTRATING HORN GROWTH

Where $df$ = Shift in resonant frequency with ice

$df_a$ = Asymptote of shift in resonant frequency with ice.

$k$ = constant

$$I = 1/k' \quad \ln(1-di/di_a) \qquad (2)$$

Where $di$ = Shift in frequency index with ice

$di_a$ = Asymptote of shift in resonant frequency with ice

$k'$ = constant

It has been found more practical to use Equation 2, however, where i, the frequency index or count generated by the computer is used in place of frequency since for every frequency index there is a corresponding value of frequency f. A measurement of di is equivalent to a measurement of df; and di, being continually generated by the computer as the ice grows, is readily available from computer memory. Curves of measured di vs measured ice thickness (e.g., Figure 8) are readily obtained from the computer printout (e.g., Figure 4) and serve as a means for calibrating the MIAMI. The calibration process consists of determining values of k' and $di_a$ that cause Equation 2 to fit the measured data. Since these terms were established from measurements on ice layers up to 125 mils Equation 2 is, rigorously, applicable only to ice layers less than 125 mils. However, since Equation 2 has been verified theoretically, it can be expected to give useful information up to the maximum, or dynamic range of the MIAMI transducer. Future tests on thicker ice layers are required to verify that the equation is applicable to thick layers.

### 2.2.2. MIAMI Indications at Temperature Near The Freezing Point

In MIAMI tests, run during June and August, a "run" or "test" was tacitly considered to be "that period between the time the spray

was turned on" and "the time it was turned off." No formal plans were made to measure ice growth history after the spray was turned off. Accordingly, it was routine procedure to turn the spray on and monitor the ice growth history with the MIAMI and a manually operated calibrated transit. It was assumed by the test crew and the transit operator that when the spray was turned off, the test was over and there was no need to continue to measure ice thickness. Accordingly, the operator of the transit ceased to make any further measurements - after the spray was turned off.

The MIAMI, however, being automatically controlled by the micro-processor, did no such thing but continued to monitor and record ice thickness and was permitted to run out its preprogrammed period of time of approximately 260 seconds. It was during this unplanned testing period after the spray was turned off that it was noted that when the air temperature was close to freezing, the MIAMI indicated an exponential like decay in ice thickness (runs 1.1 and 2.1). Since there were no independent transit measurements during this time to compare the MIAMI indications with, it is impossible to establish from the data if there actually was a loss in thickness or some other more subtle phenomenon took place (at lower temperatures this phenomenon did not manifest itself).

Various hypotheses explaining this behavior can be made - each of which must be verified by additional testing.

The simplest hypothesis explaining this behavior is that there actually was an ice loss at these temperatures. Some evidence exists (Stallabrass Ref 2) that at temperatures within about $-4^{o}c$ of freezing, the adhesive and cohesive forces of ice are weaker than they are at lower temperatures, e.g., the ice

---

Ref 2 - J.R. Stallabrass and R. D. Price, "On the Adhesion of Ice to Various Materials" National Research Laboratories, July, 1962.

structure is not as rigid or is softer than it is at lower temperatures and aerodynamic forces acting on the ice structure are sufficient to cause it to erode somewhat. As long as the spray is on and new ice is forming, the structure can maintain its growth.

A more complicated hypothesis would be the following: When the air temperature is at or slightly below freezing, it should not be expected that all of the water droplets will freeze instantaneously upon impact. Only a certain fraction will freeze on impact, forming a rigid ice structure, while the remaining fraction of the water droplets will not freeze but will be trapped or bound as unfrozen water in the ice structure that has formed. There is not sufficient heat transfer during these conditions to remove all of the latent heat from the impinging droplets so they do not freeze on impact.

If we confine our attention only to the sample volume within the field of the MIAMI, we should expect that within this volume some of the bound water in the liquid state is free to migrate or drain out of the sample volume, while simultaneously some of the bound water will freeze with time, and remain in the sample volume. As long as the spray is on new water droplets will be added to the sample volume. Some of these will freeze, increasing the size of the ice structure within the sample volume and some will migrate out of the sample volume. The liquid water migrating out of the sample volume being always less than the liquid water being added to the sample volume by the spray. The difference between the water leaving and the water added is the ice forming within the sample volume.

In summary, what we have within the sample volume in the field of the MIAMI, as long as the spray is on, is a continuously increasing ice structure containing a certain fraction of unfrozen water. If the spray is turned off so that there is no new

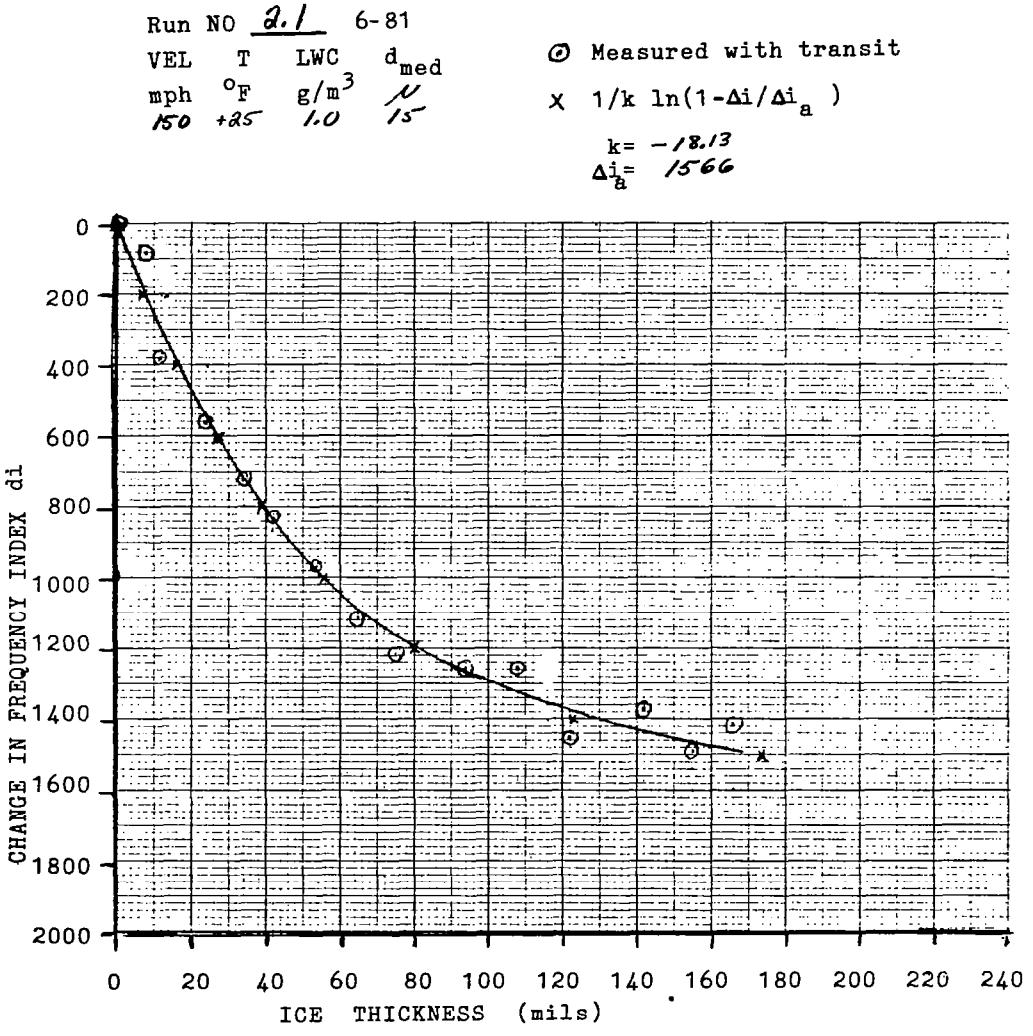


FIGURE 8 - EXPERIMENTAL CURVE OF SHIFT IN FREQUENCY INDEX VERSUS ICE THICKNESS

source of water entering the sample volume some of the liquid water will continue to migrate out but some will freeze until a point in time is reached when there is no more liquid water in the sample volume but only pure ice, or an ice-air mixture. In addition, there could be some erosion of the ice structure by aerodynamic forces.

Such an hypothesis will explain the behavior of the MIAMI observed when the air temperature was at or near freezing (runs 1.1 and 1.2). During these experiments, the MIAMI indicated linear growth of ice with time, corresponding to the growth in size of the ice-water mixture within the sample volume of the MIAMI. Since water has a higher dielectric constant than ice, the effective dielectric constant of the ice-water mixture within the sample volume should be somewhere between the two and higher than that of pure ice. When the spray is turned off and the water fraction reduces to zero (by migration of some water out of the sample volume, and the freezing of some water that remains in the sample volume), the effective dielectric constant will relax or decay, exponentially, asymptotically approaching the effective dielectric constant of the ice-air mixture remaining within the sample volume. The higher dielectric constant of the ice-water mixture will have a greater tuning effect on the MIAMI causing it to indicate thicker ice layers. As the water freezes or is otherwise removed, the indications should drop as observed.

### 2.3 Measured Dynamic Range of the MIAMI-Model No. 6

In the 15 runs made with Model No. 6 listed in Table 1, the tunnel parameters were set to produce rapid icing so that the ice thickness soon exceeded the range of the MIAMI transducer. The maximum range of the transducer was taken to be the maximum reliable reading provided by the MIAMI that was not obscured by noise. Using this criterion, the average dynamic range recorded was 210 mils.

Model No. 6 operates in the 6 Ghz frequency band. Theory (Section 3) indicates that if the operating frequency is lowered the dynamic range will increase, (e.g., if the frequency is divided by two the dynamic range will double.) Thus, larger MIAMI's should have larger dynamic ranges. Theoretically, dynamic ranges to 1 inch are not unreasonable.

TABLE NO 1 MIAMI MODEL NO 6, RUNS IN WHICH THE ICE THICKNESS EXCEEDED THE DYNAMIC RANGE OF THE MIAMI

| | RUN NO | VEL mph | $T$ °F | LWC $g/m^3$ | $d_{med}$ $\mu$ | estimated dynamic range (mils) |
|---|---|---|---|---|---|---|
| JUNE RUNS | 7.1 | 150 | 0 | 1.0 | 15 | 240 |
| | 8.1 | 150 | -10 | 1.0 | 15 | 220 |
| | 12.1 | 200 | 0 | 1.0 | 15 | 180 |
| | 13.1 | 200 | 10 | 1.0 | 15 | 220 |
| | 28.1 | 150 | 0 | 1.25 | 19 | 180 |
| | 30.1 | 150 | 0 | 1.8 | 19 | 220 |
| | 32.1 | 150 | -10 | 1.25 | 19 | 220 |
| | 34.1 | 150 | -10 | 1.8 | 19 | 200 |
| AUGUST RUNS | 18 | 150 | 20 | 1.8 | 19 | 220 |
| | 20 | 200 | 20 | 1.0 | 15 | 200 |
| | 21 | 200 | 20 | 1.5 | 20 | 220 |
| | 27 | 150 | 10 | 1.8 | 19 | 200 |
| | 29 | 200 | 10 | 1.0 | 15 | 190 |
| | 30 | 200 | 10 | 1.5 | 20 | 200 |
| | 36 | 200 | 0 | 1 | 15 | 240 |

Average dynamic range = 210 mils

## 2.4 Effect of Liquid Water on the MIAMI at Temperatures Above Freezing

As pointed out earlier one of the main features of the MIAMI is that it is flush mounted with the surface being monitored. As such, it does not interfere with the aerodynamic properties of the airfoil. Under these conditions when the surface being monitored is placed into an airstream, above freezing, with a high liquid water content, the water droplets impinging on the MIAMI will have little opportunity to accumulate on its surface. Only small droplets of water, within the boundary layer of the airstream will remain in the field of the MIAMI. These can be expected to run off quickly as their size grows.

Tests to demonstrate the MIAMI performance under these conditions were run on June 30, 1981, Run No. 28. The parameters of the IRT were set to the following values:

| | |
|---|---|
| Temperature | $47^{o}F$ |
| Air Velocity | 150 mph |
| Liquid Water Content | 1.8 $gm/cm^3$ |
| Droplet Size | 19 $\mu$ |

The computer printout and oscillogram indicate only minor, negligible, random perturbations of the MIAMI quiescent resonant frequency, as might be expected from the above hypothesis.

It is well known that water is an extremely lossy dielectric material and that any significant quantity that is permitted to accumulate in the field of the MIAMI will destroy its resonance by absorbing the stored energy. This phenomenon was noted in a number of unrecorded informal tests performed with water at room temperature. One should keep in mind, however, that the phenomenon being discussed here always take place above freezing temperatures when the MIAMI would not be expected to be operational and icing is not expected.

## 3.0 MIAMI DESIGN THEORY

### Theoretical Basis for the MIAMI

The theoretical basis for the MIAMI is that the resonant frequency of a resonant surface waveguide is altered or tuned by the growth of ice on it. An oscillogram illustrating and verifying this phenomena is shown is Figure 5a for MIAMI Model No. 6.

If the shift in resonance caused by ice of known thickness is measured an empirical relation between ice thickness and frequency shift can be established which, from then on, can be used to measure the ice thickness from a measurement of the frequency shift. A typical curve of ice thickness vs frequency shift is shown in Figure 8 for MIAMI Model No. 6.

The MIAMI transducer consists of a resonant surface waveguide on which the ice is permitted to accrete and instrumentation which continually monitors its resonant frequency and converts the measured change in frequency to ice thickness by means of the empirical equation illustrated in Figure 8 and described by Equation 2. The surface waveguide is composed of a layer of stable dielectric material such as polyethelene which has approximately the same dielectric constant as ice and is placed just under the surface on which ice is to be measured as illustrated in Figure 9.

In the ice free condition, the surface waveguide is made resonant by making its length equal to an integral number of half wavelengths. As layers of ice begin to form on the dielectric surface of the waveguide, they have the effect of thickening the waveguide and altering its resonant frequency.

### Properties of a Polyethelene Surface Waveguide

The properties of a polyethelene surface waveguide may be established from a plot of guide wavelength versus frequency for

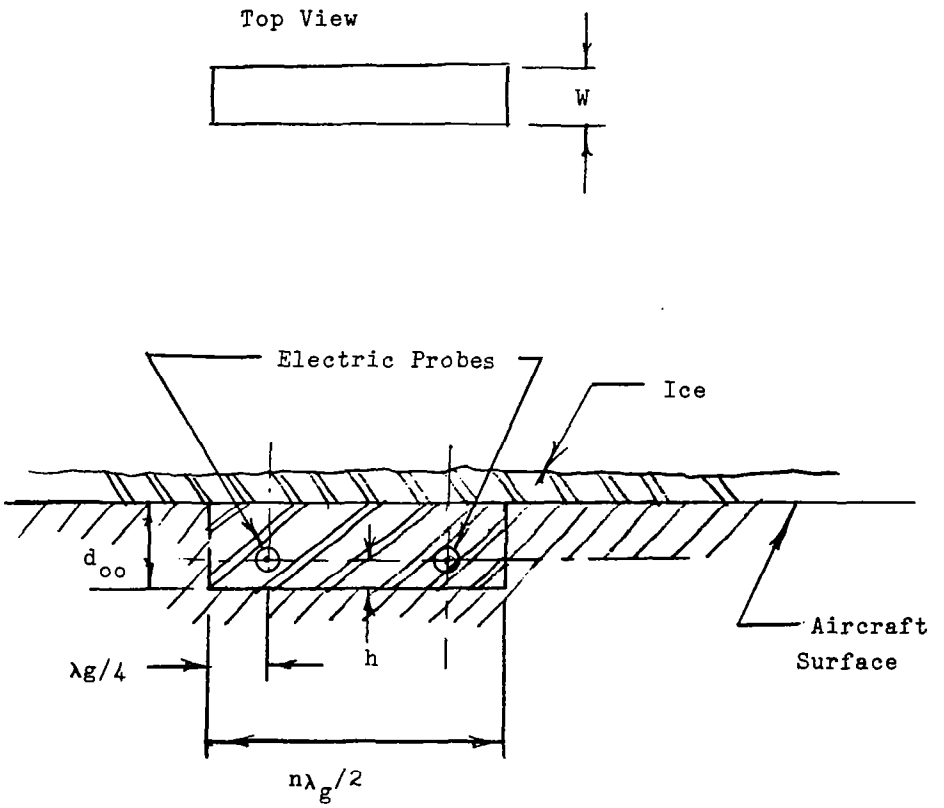


FIGURE 9 - DIAGRAM ILLUSTRATING CONSTRUCTION OF MIAMI TRANSDUCER

various thicknesses of the surface waveguide as illustrated, in Figure 10, between 1 and 2 Ghz for the $TE_1$ mode. This is obtained by techniques outlined in Ref. 3.

Similar plots made over other octave bands such as 2 to 4 and 4 to 8Ghz, etc., reveal that all plots are identical if the scales are related by a normalization factor p so that Figure 10 may be used to represent any octave band given the normalization factor.

Referring to Figure 10, the surface waveguide of thickness d is made resonant by making its length equal to an integral number of half wavelengths. Thus, from Figure 10 when dp=8 cm. and f/p=1.66 Ghz (point a Figure 10), the surface waveguide is resonant when its length $p \times \lambda_g = 14.2$ cm. This is defined here as the quiescent resonant frequency, foo.

The growth of ice layers, assuming the ice has approximately the same dielectric constant as the base dielectric, has the effect of increasing the thickness d of the surface waveguide. As seen from Figure 10, this has the effect of decreasing the wavelength for a given frequency and destroying the resonance. The condition of resonance is restored by increasing the wavelength by decreasing the frequency until the wavelength is once again equal to the guide wavelength that existed in the ice free condition. The tuning process is illustrated in Figure 10 as the locus of points along the horizontal line of constant $\lambda_g$ .

---

Ref. 3 - Feasibility Analysis for a Microwave Deicer for Helicopter Rotor Blades USAAMRDL-TR-76-18, May 1977, By: Bertram Magenheim and Frank Hains.

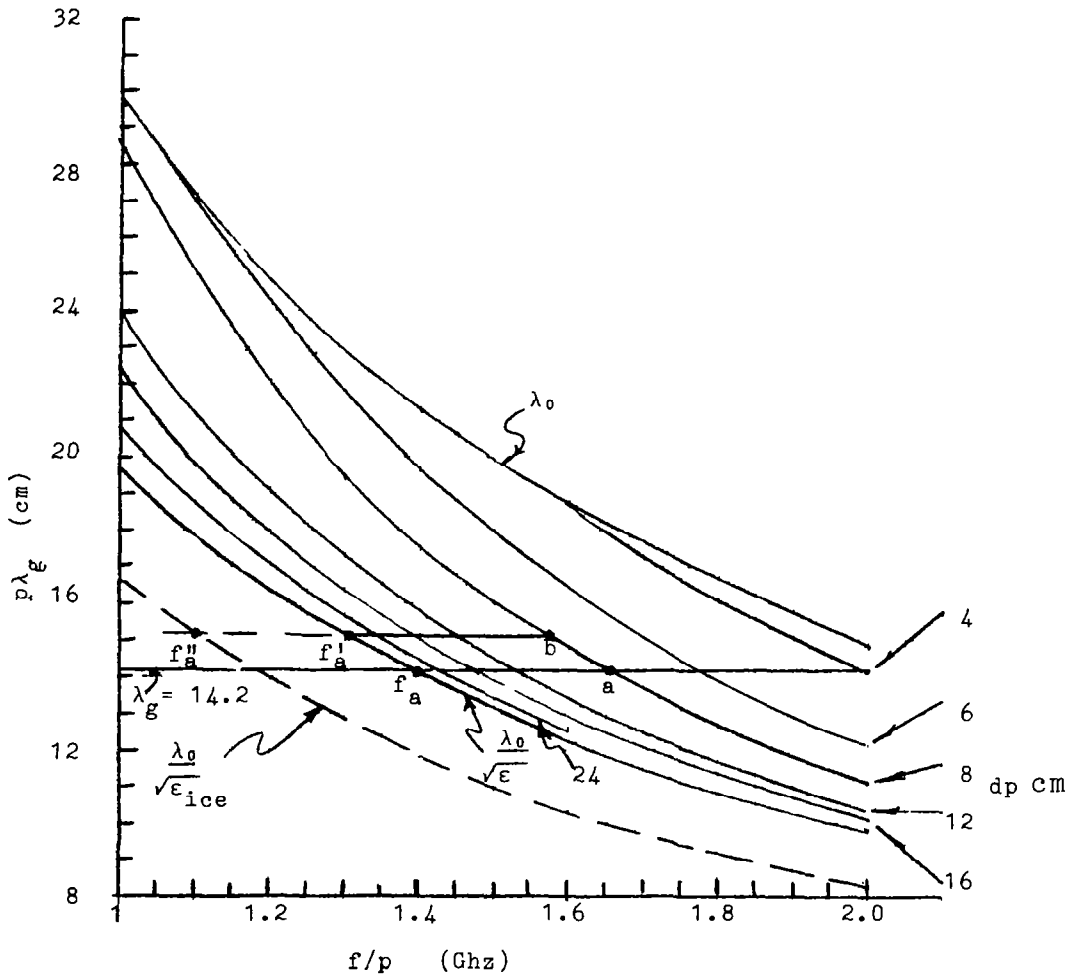


FIGURE 10 - NORMALIZED PLOT OF GUIDE WAVELENGTH VERSUS FREQUENCY

First Order Approximation of the MIAMI Tuning Curve

The first order approximation of the tuning curve is obtained from this locus described above by making a table of f/p versus dp with p x $\lambda g$ held constant. The approximation is illustrated in Figure 11(a). The curve of Figure 11(a) appears to be a descending exponential and can be very closely approximated by eq (3) which is similar to eq (1). (Second approximation Figure 11(b) is discussed in Section 3.2.)

$$x = 1/k \ln (1-y/y_a) \qquad (3)$$

Where:

$x$ = d(d p)

$y$ = d(f/p)

$y_a$ = Asymptote of y = 0.5417

$k$ = constant = 0.268

3.1 Choosing MIAMI Dimensions

The dimensions chosen for the experimental MIAMI were based on the following considerations:

- small size
- widest dynamic range
- sensitivity
- available oscillator tuning range
- oscillator cost
- ruggedness and reliability.

The voltage tuned oscillator (VTO) chosen was the Avantek Model 8580 that tunes a 12% band from 5.8 Ghz to 6.6 Ghz. This is a low cost VTO which, because of its frequency band, would permit construction of a small MIAMI transducer. Two designs making use of this VTO were prepared, Model No. 5 and 6. Tuning curves for these models were plotted on the normalized tuning curve and are illustrated in Figure 12. Model no. 5 with p = 3.3 occupies the higher sensitivity but lower dynamic range portions of the

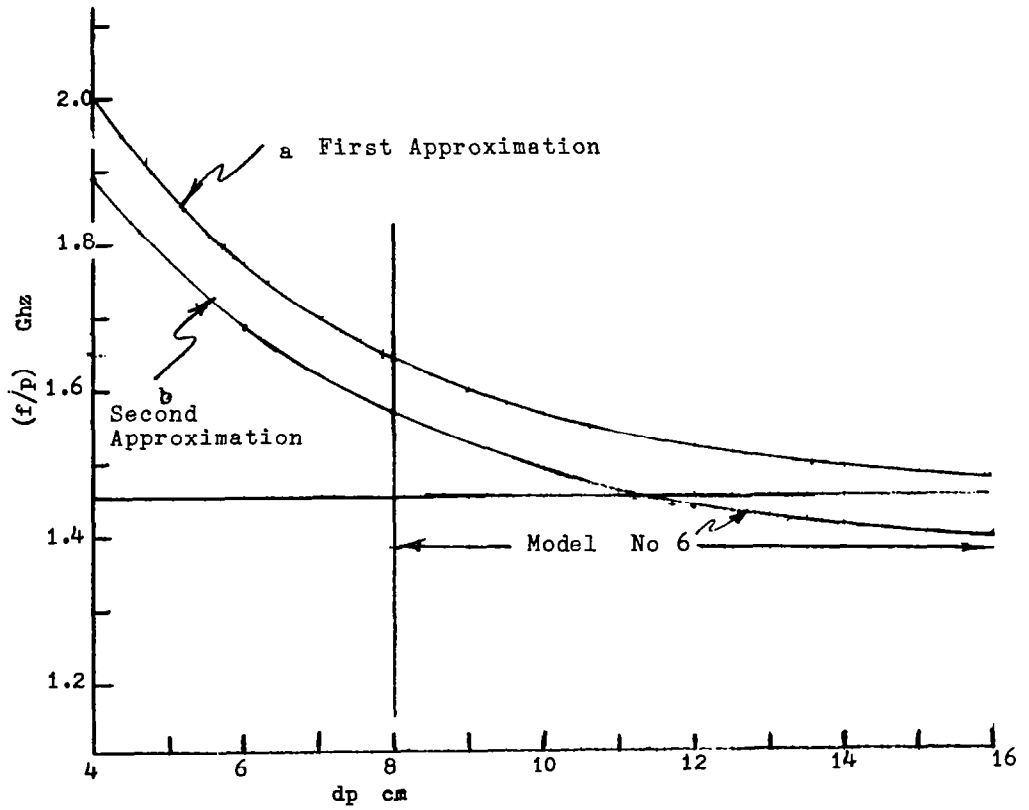


FIGURE 11 - NORMALIZED TUNING CURVE OF MIAMI FIRST AND SECOND APPROXIMATIONS

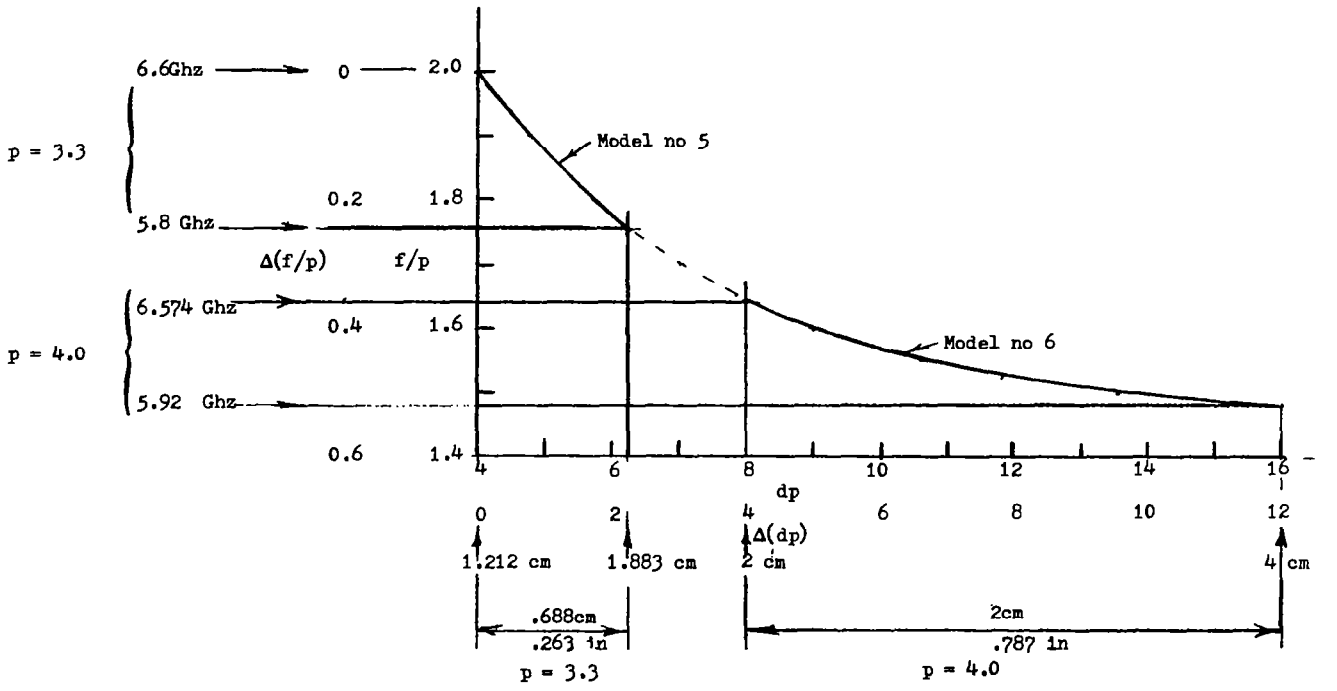


FIGURE 12 - NORMALIZED TUNING CURVE OF MIAMI FIRST APPROXIMATION. MODELS 5 AND 6 ILLUSTRATED

tuning curve whereas Model no. 6, p = 4 occupies the lower sensitivity but higher dynamic range portion of the tuning curve. The theoretical dimensions of Models 5 and 6 are summarized below.

| Model No. | p | Freq. Range | Cut-off freq. | Length a | Depth b | Width c | Dynmc Range | Sensitivity |
|---|---|---|---|---|---|---|---|---|
| | | Ghz | Ghz | inch | inch | inch | inch | Ghz/in |
| 5 | 3.3 | 5.8<br>6.6 | 5.42 | 1.694 | .477 | .250 | .263 | 5.89 to<br>3.726 |
| 6 | 4 | 5.92<br>6.57 | 3.28 | 1.398 | .787 | .25 | .787 | 1.96 to<br>.224 |

### 3.2 Construction and Test of Experimental Surface Wave-Guides

Both Model 5 and 6 were constructed and tested. The measured resonance curve for Model 5 proved to be non-uniform and unstable possibly because of its proximity to cut-off. Model 6 proved to be far more tractable; it demonstrated a smooth resonance curve capable of being tuned by layers of polyethelene tape as illustrated in the measurements of Figures 13 to 16.

The ideal way to tune and calibrate the MIAMI would be to place ice layers of precisely known thickness and shape on the MIAMI surface; but because of the practical difficulty of doing this in the laboratory, at room temperature, the ice layers were simulated by adding layers of polyethelene tape of known thickness to the MIAMI. Because the tape may be added one layer at a time, it could be made to conform to the shape of the MIAMI surface as well as serve as a thickness gauge. Table 2 summarizes the tuning data taken from Figures 13 to 16.

The quiescent (no ice) resonant frequency of Model No. 6 differed from its theoretical value being approximately 6.29 Ghz rather than 6.6 Ghz. This is because the end plates of the transducer are not perfect short circuits as assumed in the first order

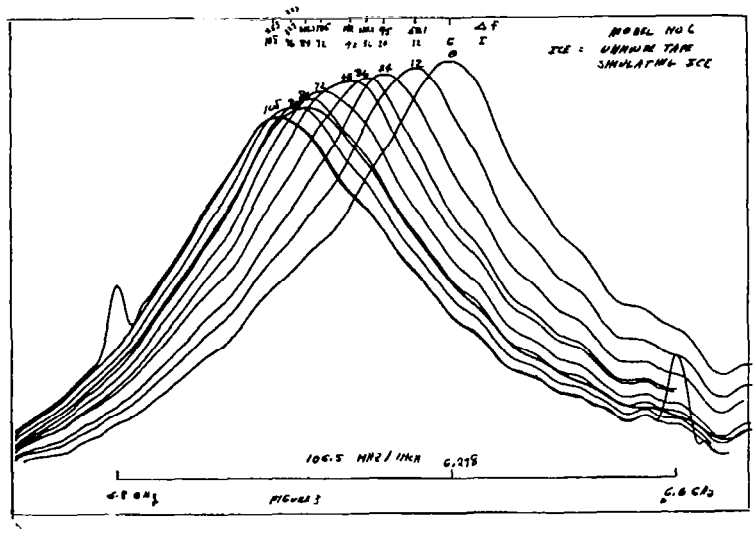

FIGURE 13 - PEN RECORDING - MODEL NO. 6 - MEASURED SHIFT IN RESONANCE DUE TO LAYERS OF POLYETHELENE TAPE

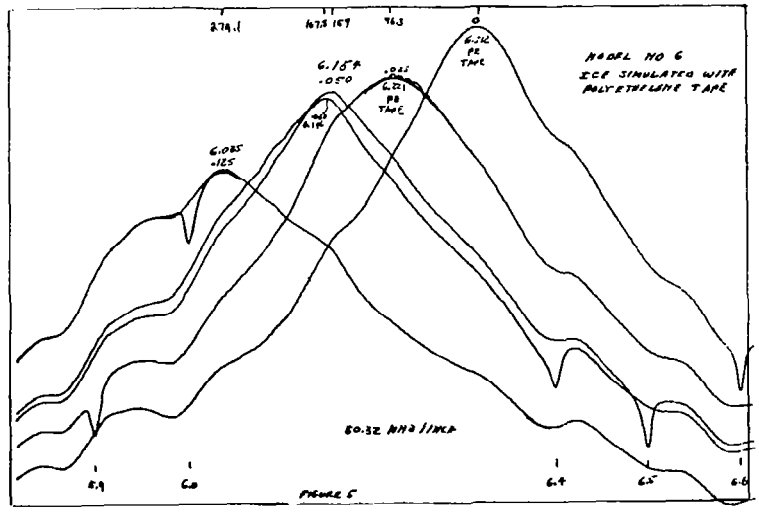

FIGURE 14 - PEN RECORDING - MODEL NO. 6 - MEASURED SHIFT IN RESONANCE DUE TO LAYERS OF POLYETHELENE TAPE

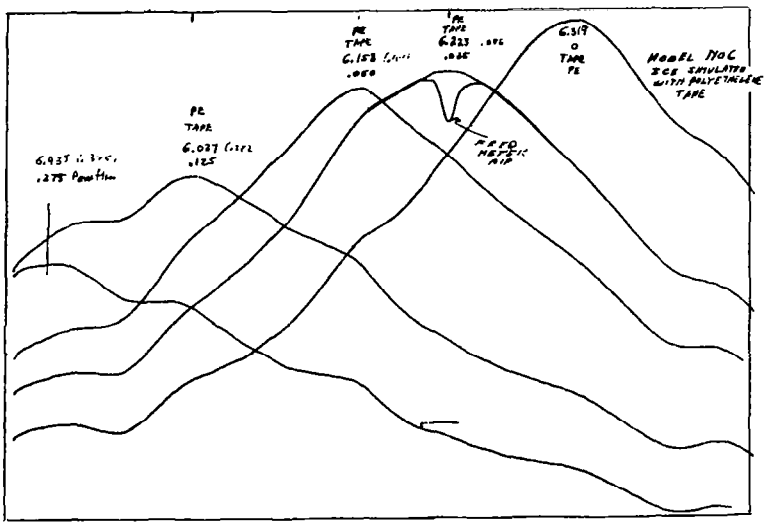


FIGURE 15 - PEN RECORDING - MODEL NO. 6 - MEASURED SHIFT IN RESONANCE DUE TO LAYERS OF POLYETHELENE TAPE

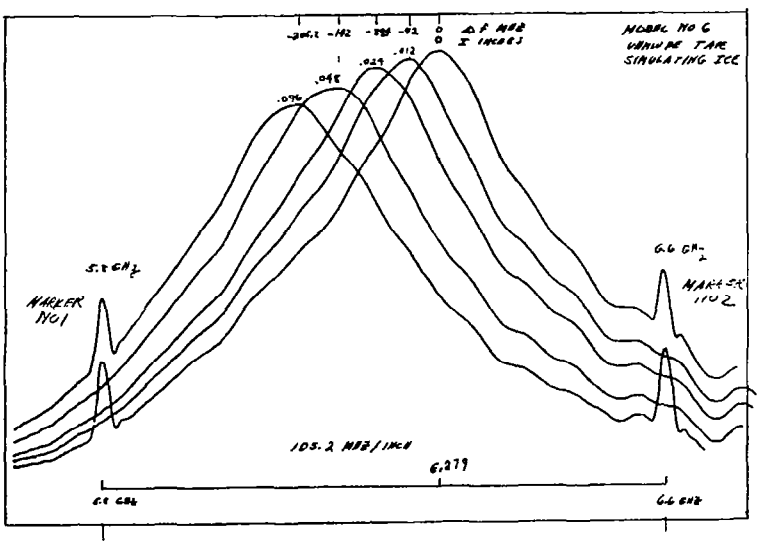


FIGURE 16 - PEN RECORDING - MODEL NO. 6 - MEASURED SHIFT IN RESONANCE DUE TO LAYERS OF POLYETHELENE TAPE

Table 2- Tuning Data Ice Simulated by Polyethelene

| Fig No | d(i) | d(f) Ghz | d(d) mils | d(d) cm | d(f/p) Ghz | d(dp) cm |
|---|---|---|---|---|---|---|
| 13 ⊙ | 0 | 0 | 0 | 0 | 0 | 0 |
| | 180 | .042 | 12 | .0304 | .0105 | .1216 |
| | 365 | .0894 | 24 | .061 | .0224 | .244 |
| | 540 | .142 | 48 | .122 | .0355 | .488 |
| | 740 | .205 | 96 | .244 | .0513 | .975 |
| 14 △ | 0 | 0 | 0 | 0 | 0 | 0 |
| | 215 | .0501 | 12 | .0304 | .0125 | .1216 |
| | 380 | .095 | 24 | .061 | .0224 | .244 |
| | 469 | .120 | 36 | .091 | .0300 | .366 |
| | 545 | .142 | 48 | .122 | .0355 | .488 |
| | 680 | .185 | 72 | .183 | .046 | .732 |
| | 740 | .205 | 84 | .213 | .0514 | .853 |
| | 805 | .227 | 96 | .244 | .057 | .975 |
| | 880 | .253 | 108 | .274 | .063 | 1.096 |
| 15 ⊡ | 0 | 0 | 0 | 0 | 0 | 0 |
| | 388 | .096 | 25 | .064 | .024 | .254 |
| | 602 | .161 | 50 | .127 | .040 | .508 |
| | 991 | .282 | 125 | .318 | .071 | 1.27 |
| | --- | .384 | 275 | .699 | .096 | 2.79 |
| 16 X | 0 | 0 | 0 | 0 | 0 | 0 |
| | 388 | .096 | 25 | .064 | .024 | .254 |
| | 600 | .159 | 50 | .127 | .0398 | .508 |
| | 625 | .168 | 60 | .152 | .0419 | .610 |
| | 955 | .279 | 125 | .318 | .0697 | 1.27 |

theory. They are slightly inductive and have the effect of electrically lengthening the surface waveguide. Therefore, its quiescent resonant frequency is lower than would be computed from consideration of the physical length of the guide alone. The adjustment in quiescent resonant frequency is illustrated in Figure 10 (a to b) and a second approximation of the tuning curve obtained due to this adjustment is illustrated in Figure 11(b).

The portion of the curve occupied by Model No. 6 is indicated on Figure 11(b). This portion has been replotted in Figure 17 $fa'$ with coordinates d (f/p) for ordinate and d(dp) for absissa.

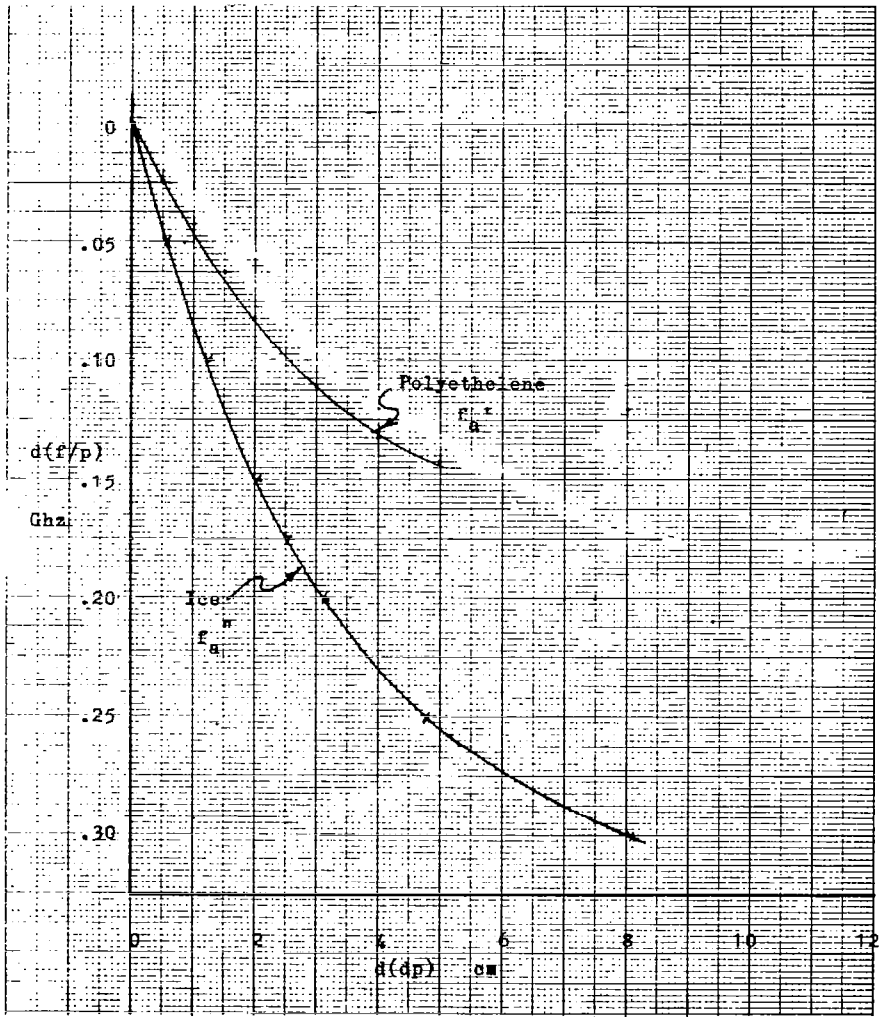


FIGURE 17 - NORMALIZED - THEORETICAL TUNING CURVE - MODEL NO. 6 - SECOND APPROXIMATION

### 3.3 Agreement Between Theory and Experiment Measured Tuning Curves

Tuning curves for Model No. 6 were measured using simulated and real ice as tabulated below.

| Figure | Symbol | Dielectric Used | Dielectric Constant | Temp | Location |
|---|---|---|---|---|---|
| 13 | ⊙ | Polyethelene | 2.3 | room | lab |
| 14 | △ | " | 2.3 | room | lab |
| 15 | ⊡ | " | 2.3 | room | lab |
| 16 | × | " | 2.3 | room | lab |
| 18 | | Ice | 3.2 | Freezing | Wind Tunnel |

The resulting curves (normalized) are illustrated in Figure 18 where they are compared with the theoretical curve (second approximation) for polyethelene. The theoretical curve for polyethelene is the same as Figure 17 fa'. The tuning curve for ICE was obtained experimentally being the average of 33 test runs in June, in the NASA Lewis Icing Research Tunnel (IRT).

The theoretical curve for ice may be estimated. Since ice has a higher dielectric constant than polyethelene (3.2 vs 2.3) it will have a greater tuning effect on the MIAMI. An estimate of the ice asymptote may be obtained from Figure 10 if the limiting curve for ice, $\lambda_g = \lambda_o/\sqrt{\varepsilon}$ ($\varepsilon$ = 3.2 for ice) is also plotted and the intersection of $\lambda_g$ and this curve established fa" in Figure 10. The ratio of theoretical dynamic ranges being from Figure 10.

$$\frac{d(f/p)_{aI}}{d(f/p)_{ap}} = \frac{b-f''_a}{b-f'_a} = \frac{0.47}{0.27} = 1.74$$

This establishes d(f/p)aI for use in the empirical equation eq 3 from which the theoretical curve for ice is established in Figure 18 and 17.

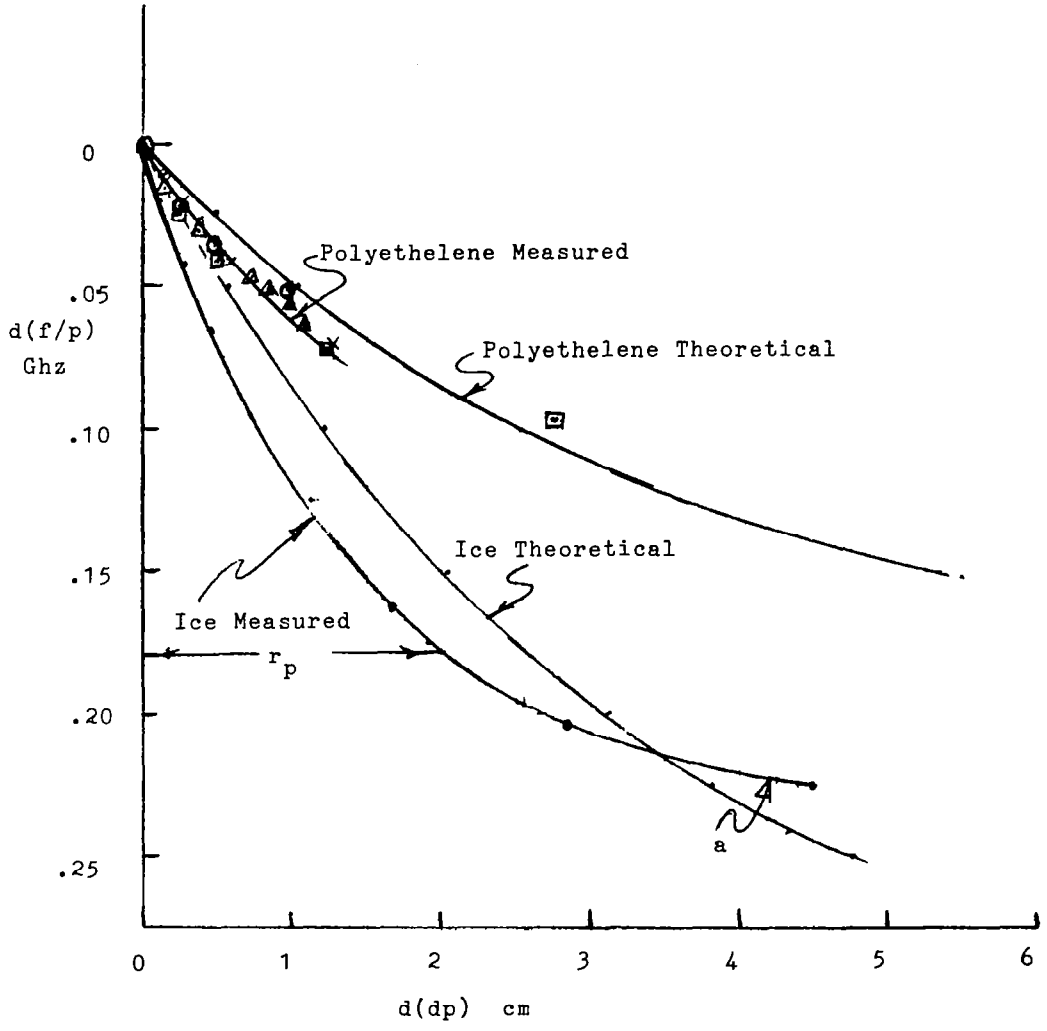


FIGURE 18 - COMPARISON OF THEORETICAL DATA (SECOND APPROXIMATION) AND MEASURED DATA ON NORMALIZED COORDINATES MODEL NO. 6

Where d(f/p)aI = Dynamic range for ice
d(f/p)ap = Dynamic range for polyethelene.

The difference between the first order approximation for polyethelene and measured polyethelene is that the approximation assumes the impedance of the end plates of the waveguide does not vary as layers of polyethelene are added whereas in reality the impedance of the end plates does vary. Similarly, for ice, the impedance of the end plates changes as ice is added and since ice has a higher dielectric constant than polyethelene the effect is even more pronounced.

### 3.4 Coupling to the Surface Waveguide (Simplified Theory)

The probes used to couple energy into the resonant surface waveguide were designed intentionally to provide very light coupling so that a high loaded Q with very little radiation would be realized. The probes couple energy to the electric fields in the surface waveguide and, therefore, the coupling efficiency is dependent upon the relative strength of the electric field at the location of the probe. The coupling is zero at frequencies below cut-off of the surface waveguide but starts to rise as the operating frequency is increased above cut-off. Trying to operate a MIAMI at frequencies only slightly above cut-off while yielding very high theoretical sensitivity is impractical because the coupling will be too low. The operating frequency must be sufficiently above cut-off to provide adequate but light coupling. The coupling is also a function of the height of the probe relative to the thickness of the dielectric; h/d, as shown in Figure 9 (d = doo, when no ice exists h is the height of the probe above the bottom of the surface waveguide.) Since the electric field at the probe decreases as d increases the coupling will, therefore, decrease as ice accretes since this is equivalent to decreasing h/d. The probe was placed a quarter wavelength from the end plate since this dimension is independent of ice thickness and frequency (guide wavelength in a resonant surface waveguide is constant). There is no variation in coupling due to this dimension.

## 4.0 THE MIAMI SYSTEM THEORY

A block diagram of the MIAMI System is shown in Figure 19. The microprocessor is programmed to generate a repetitive count (i) down from the number 2047 to zero. The count, a number generated by the microprocessor, is also called the frequency index. The count is converted in the digital to analog converter (DAC) to an analog voltage (Vi). This voltage appears as a negative going sawtooth the amplitude of which is directly proportional to the count. This voltage is transmitted to the MIAMI transducer via a long multiconductor cable where it is amplified and used to sweep the voltage tuned oscillator (VTO) through its frequency range. Each count or number generated by the microprocessor corresponds to a different frequency output (f) of the VTO. The microwave signal generated by the VTO is then passed through the resonant surface waveguide whose resonant frequency (fo) is a function of the ice thickness. The signal is then detected by the crystal detector. The voltage out of the crystal detector (Vo) is then amplified and transmitted via the long multiconductor cable to the analog to digital converter where it is converted into a digital number (Ai). A peak sensing algorithm in the microprocessor then determines the frequency index (count) that produced a peak output of the resonant surface waveguide. This is called the resonant frequency index.

In the ice free condition, the resonant frequency is called the quiescent resonant frequency, foo. The resonant frequency index that generated the quiescent resonant frequency is called the quiescent frequency index, (ioo). When ice forms on the transducer, tuning the surface waveguide, the resonant frequency index decreases in value. The difference between the quiescent frequency index, ioo, and the resonant frequency index, io, is a function of ice thickness.

The functional relationship between ice thickness and frequency index is established experimentally and stored in the microprocessor. The microprocessor then continually monitors the

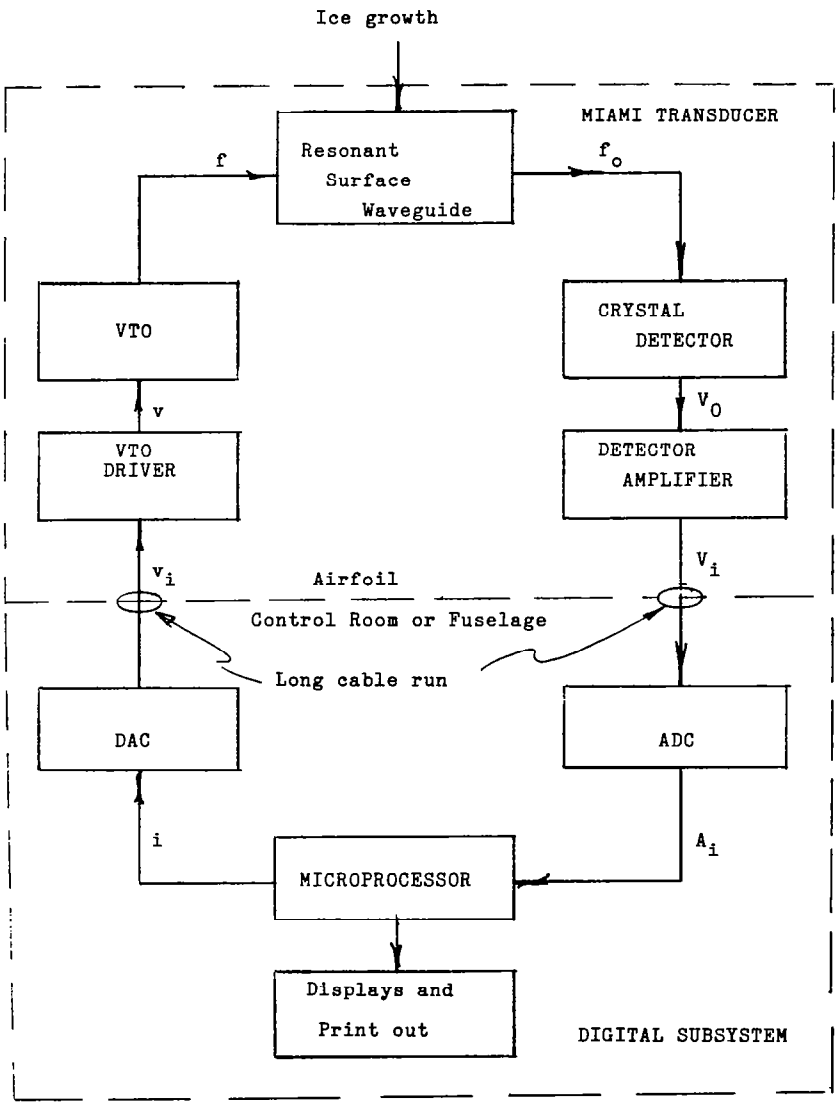


FIGURE NO 19 - MIAMI SYSTEM BLOCK DIAGRAM

change in frequency index and using the stored function calculates the ice thickness. The microprocessor then computes the accretion rate of the ice by calculating the first time derivative of ice thickness. These values are then available for subsequent display.

### 4.1 Theoretically Derived Relation Between Ice Thickness and Frequency Index

The relationship between frequency index and ice thickness may be obtained functionally from Figure No. 19 provided the transfer constants of the surface waveguide as a function of ice, the VTO, the VTO driver and DAC are known. All of these transfer characteristics can be measured and derivation of their values and functional relationships appear in Appendix No.1

From eq (1) the ice thickness is a function of the shift in resonant frequency.

$$I = 1/k \ \ln(1-df/df_a) \tag{4}$$

The VTO tuning curve is represented by

$$f = f_a - f_m e^{gv} \tag{5}$$

and the transfer characteristics of the DAC and VTO driver are

$$v = mi + b \tag{6}$$

and

$$dv = m\ di \tag{7}$$

from which it can be shown that df is related to di by

$$df = f_m e^{gv_{oo}} (e^{-gmdi} - 1) \tag{8}$$

Thus, the ice as a function of di can be obtained from eq 4 and 8 as

$$I = 1/k \ln \left[ 1 - \frac{f_m e^{gV_{oo}} (e^{-gm\ di} - 1)}{df_a} \right] \qquad (9)$$

Parameters in eqs 4 to 9 are defined in the following table:

| Where | | | Poly. Theoretical | Poly. Measured | Ice Theoretical | Ice Measured |
|---|---|---|---|---|---|---|
| df | = | frequency shift | | | | |
| di | = | index shift | | | | |
| dfa | = | frequiency asymptote | 0.82 | 0.354 | 1.4268 | .573 |
| k | = | constant | -2.5 | -11.45 | -2.5 | -9.51 |
| foo | = | quiescent frequency | 6.29 Ghz | | | |
| fm | = | VTO parameter | 1.30 | | | |
| g | = | VTO parameter | -0.0735 | | | |
| m | = | slope of VTO driver | 0.0058 | | | |
| Voo | = | quiescent VTO voltage | 11.68 | | | |
| e | = | base of natural log | | | | |

Figure 20 was prepared to illustrate the agreement between the theoretically derived eq 9 and measurements. Four plots of eq 9 are shown for:

Ice measured
Ice theoretical
Polyethelene measured
Polyethelene theoretical.

Parameters of the MIAMI components tabulated above do not change in any significant manner compared to the shift in resonant

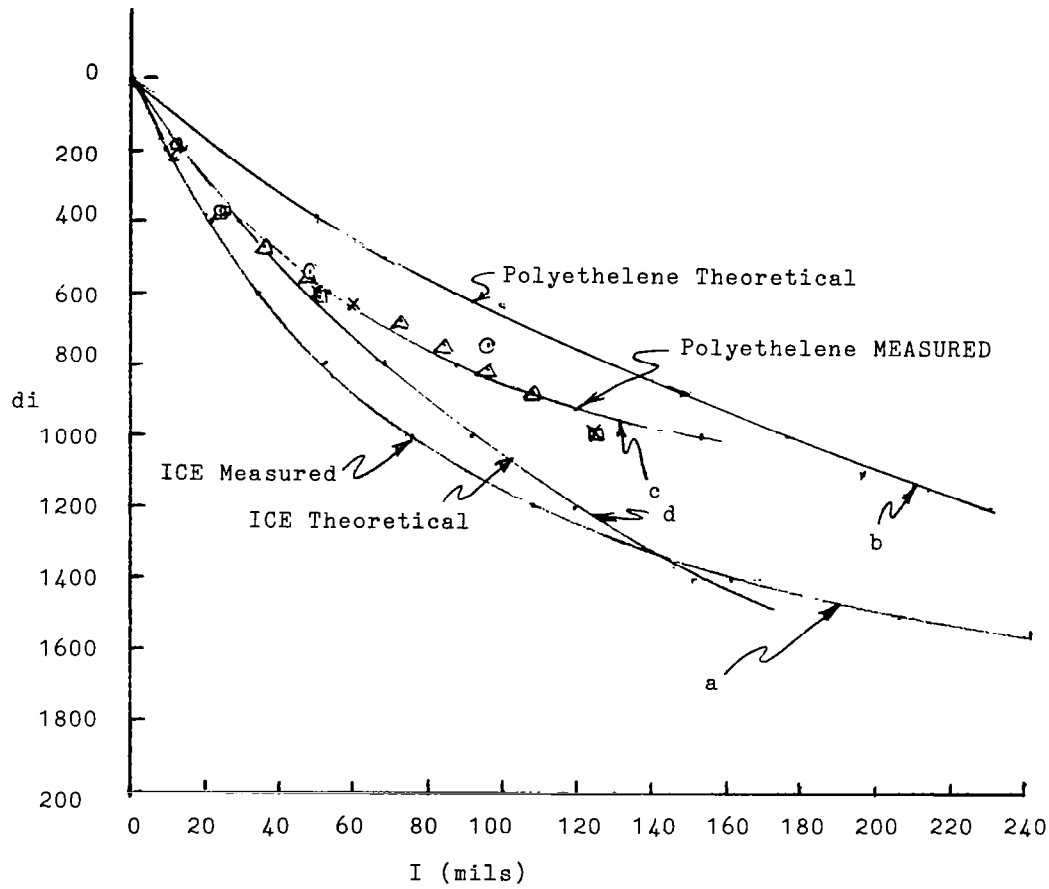


FIGURE 20 - COMPARISON OF THEORETICAL AND EXPERIMENTAL DATA OBTAINED WITH MATHEMATICAL MODEL OF MIAMI SYSTEM

frequency index. The microprocessor monitors changes in index (di) not absolute values of index (i) so that the effect of changes in foo or ioo with ambient temperature are minimized. All component parameters tabulated above were established experimentally.

### 4.2 Variation of Dynamic Range with MIAMI Dimensions

The dynamic range of the MIAMI system is limited primarily by the design of the MIAMI transducer. The dynamic range for a particular transducer can be established from its tuning curve. The tuning curve for Model No. 6, as measured during tests performed in June 1981, is illustrated in Figure 18a on normalized coordinates. The practical normalized dynamic range is indicated as "rp" on Figure 18a (r is the dynamic range, p is the normalization factor). The dynamic range is defined here as the ice thickness indicated by the MIAMI when the resonant frequency of the MIAMI has shifted to a value equal to 80% of the frequency asymptote (in Figure 18a the value of normalized dynamic range, (rp) is 2.0 cm when d(f/p) is 0.180 Ghz which is approximately 80% of the asymptote of d(f/p) which is about 0.225).

The dynamic range thus defined is useful in that it is a number representing the order of magnitude of ice thickness that can be accurately read by the MIAMI. The arbitrarily chosen 80% criterion may be more conservative than necessary since it may be possible to obtain accurate readings from the MIAMI when the frequency shift is closer to the asymptote.

Thus, using a conservative normalized dynamic range rp of 2.0 cm, the following table shows how the absolute value of dynamic range, r, varies as the normalization factor, p, is varied.

Variation in Dynamic Range, r, with Normalization Factor, p, established from MIAMI Model No. 6.

| Normalization Factor | Dynamic Range if rp =2cm | | Quiescent Resonant Frequency | Thickness of Surface Waveguide | | |
|---|---|---|---|---|---|---|
| p | r cm | r in | foo Ghz | doo in | doo cm | |
| 0.5 | 4 | 1.57 | 0.787 | 6.29 | 16 | |
| 1 | 2 | .787 | 1.573 | 3.149 | 8 | |
| 2 | 1 | .393 | 3.145 | 1.574 | 4 | |
| 4 | 0.5 | .196 | 6.29 | 0.787 | 2 | Measured |

Physically, the dynamic range is limited by the following considerations. The low end of the tuning range becomes useful only when the operating frequency is far enough above cut-off for the coupling efficiency to be sufficiently high to couple useful energy into the surface waveguide. The high end of the tuning curve becomes useless when the asymptote is approached and a small change in ice thickness produces only an unmeasurable change in resonant frequency.

This table shows that the dynamic range of the MIAMI may be adjusted upwards or downwards to accomodate the particular ice measurement at hand.

This table shows that when the normalization factor, p, is halved, the dynamic range doubles. The normalization factor used in the design of Model No. 6 was p=4, and ice thickness readings to at least 0.200 (0.196) were recorded. The above table shows that if the normalization factor is dropped from 4 to 1, the dynamic range will increase from 0.196 inches to 0.787 inches with a

corresponding increase in MIAMI depth doo from 0.787 inches to 3.149 inches. The quiescent frequency foo would aecrease from 6.29 Ghz to 1.573 Ghz.

## 5.0 RECOMMENDATION

It is recommended that a program be initiated that will improve, miniaturize and ruggedize the Microwave Ice Accretion Measurement Instrument (MIAMI), so that it can be mounted on a rotating cylinder and, in a later program, on fixed or rotary wing aircraft for research purposes. It will answer questions raised concerning the dynamic range, and the effects of unfrozen water and other liquids on MIAMI performance.

### Calibration and the Effects of Unfrozen Water

An ideal way to calibrate the MIAMI is to mount it on a rotating cylinder since ice will accrete uniformly in a predictable and easily measured manner on this surface.

The installation will be used for the following purposes:

1. Calibration of the Miami.
2. Determination of the MIAMI dynamic range.
3. Establish the relationship between dynamic range, operating frequency, and MIAMI size.
4. Determine the effects of unfrozen water on MIAMI's performance.
5. Measure the unfrozen water content of the ice.
6. Measure the variation in unfrozen water content with time (a transient phenomena).
7. Improve system software.

### Mounting of the MIAMI on Aircraft Surfaces

Once the improved MIAMI transducer is calibrated it may, at some later time, be transferred to either a fixed or rotary wing aircraft for the study of the effects of naturally occurring ice on aircraft performance and general research into the icing phenomena and cloud research.

Many dangerous icing encounters are transient in nature and disappear before they can be measured. With an installed MIAMI, a complete history of every icing encounter can be objectively recorded.

## 6.0 LIST OF SYMBOLS

| Symbol | Definition |
|---|---|
| di | Shift in index |
| w | Width of MIAMI transducer |
| k, k' | A constant used in empirical calibration curve |
| f | Frequency |
| df | Change in resonant frequency |
| $df_a$ | Asymptote of change in resonant frequency |
| I | Ice thickness |
| dI/dt | Accretion rate |
| i or j | Frequency index (used interchangeably) |
| di or dj | Change in frequency index |
| $di_a$ or dja | Asymptote of change in resonant frequency |
| foo | Quiescent resonant frequency |
| fo | Resonant frequency |
| ioo or joo | Quiescent frequency index |
| $i_o$ or jo | Resonant frequency index |
| T | Temperature |
| $d_{med}$ | Droplet size |
| LWC | Liquid water content |
| VEL | Airspeed |
| d | Thickness of surface waveguide |
| doo | Thickness of surface waveguide used in transducer which is resonant at foo |
| $\lambda_o$ | Free space wavelength |
| $\lambda g$ | Guide wavelength of surface waveguide |
| $\lambda_{go}$ | Guide wavelength of quiescent resonant frequency |
| p | Normalization factor |
| TE | Transverse electric |
| Ghz | Giga - Hertz |
| g | Parameter of VTO |

| Symbol | Definition |
|---|---|
| m | Parameter of VTO |
| Voo | Quiescent VTO voltage |
| e | Base of natural logorithm |
| fm | Parameter of VTO |
| r | Dynamic range of MIAMI |
| Q | Quality factor of a resonant device (ratio of energy stored to energy dissipated) |

# APPENDIX 1

## 1.0 TRANSFER CHARACTERISTICS OF DAC AND THE VTO DRIVER

The output voltage of the VTO driver amplifier is a linear function of the frequency index j (j is used interchangeably with i.)

$$v = mj + b \qquad (9)$$

where m and b have been established experimentally for Model No. 6

$m = 0.0058$ volts per index

$b \approx 2.75$ volts.

## 2.0 TRANSFER CHARACTERISTICS OF VTO 8580 MEASURED

$$f = f_a - f_m e^{gv} \qquad (10)$$

Where

$f$ = frequency output of VTO in GHz

$f_a$ = asymptote of VTO tuning curve = 6.85 GHz

$f_m$ = y intercept of VTO tuning curve when plotted on semi log paper = 1.3

$g$ = slope of VTO tuning curve when plotted on semi log paper = -0.0735

note:

Power output of VTO 8580

$P_i$ = 5mw $\pm$ 1.5 db

When $f$ = 6.6 Ghz, $V$ = 24.0 volts

## 3.0 FREQUENCY TRANSFER CHARACTERISTICS OF VTO (DERIVATION)

3.0.1 The following diagram represents the theoretical tuning curve of a varactor tuned oscillator

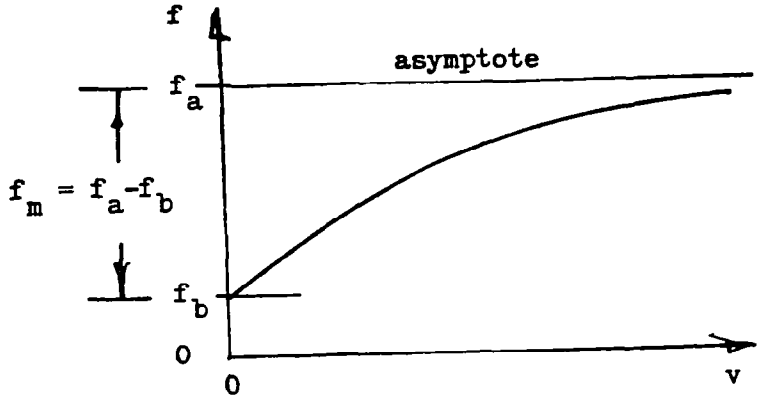


$$f = f_a - f_m e^{gv} \qquad (11)$$

when $v = \infty$

$e^{gv} = 0$ (since g is negative)

$f = f_a$

when $v = 0$

$e^{gv} = 1$

$f = f_b = f_a - f_m$

solving eq(11) for g

$$g = \frac{\ln \ (f_a - f)/f_m}{V} \qquad (12)$$

rewriting eq (11)

$$(f_a - f) = f_m e^{gv} \qquad (13)$$

$$\ln (f_a - f) = gv + \ln f_m \qquad (14)$$

equation (14) is the equation of a straight line on semi log paper with slope = g and y intercept = $\ln f_m$ as illustrated in the following diagram.

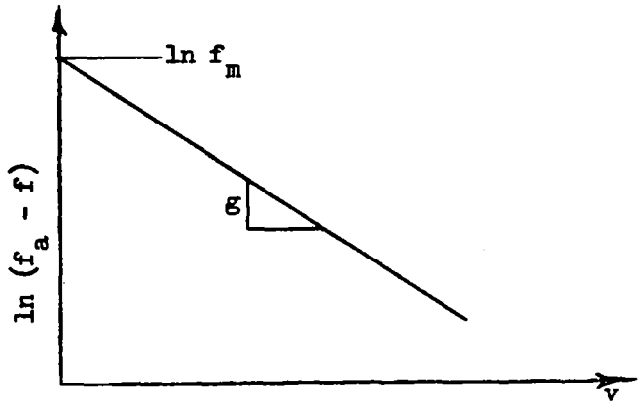


To fit the experimental data to the equation, eq (11).

1. Estimate the value of the asymptote $f_a$ by plotting experimental tuning data on rectangular coordinate paper as in Fig. 21.

2. With initial value of asymptote $f_a$ plot eq(14) on semi log paper Figure 22. The plot should be a straight line. If all points fall on the straight line, the initial value of $f_a$ chosen was a good approximation. If values do not fall on the line, choose values for $f_a$ by trial and error until all points fall on the line as illustrated in Figure 22. The highest frequency point closest to the asymptote will be the most sensitive to variations in $f_a$ when this point falls on the line the approximation is very close. The following is a table summarizing the successive estimates of fa.

TABLE SUMMARIZING THE SUCCESSIVE ESTIMATES OF $f_a$

| Manufacturers Experimental Data | | | | | | |
|---|---|---|---|---|---|---|
| Tuning voltage v volts | Output frequency f GHz | Succesive estimates of $f_a$ (Ghz) 1 6.725 | 2 6.75 | 3 6.80 | 4 6.85 | |
| | | $f_a$ - f | | | | g eq(12) |
| 5.0 | 5.8 | 0.925 | 0.950 | 1.00 | 1.05 | -0.0713 |
| 10 | 6.15 | 0.575 | 0.60 | 0.65 | 0.7 | -0.0763 |
| 20 | 6.51 | 0.215 | 0.24 | 0.29 | 0.34 | -0.0740 |
| 30 | 6.68 | 0.045 | 0.070 | 0.12 | 0.17 | -0.0725 |
| | | | | | | $g_{av}$ -0.0735 |

3. The final constants of the previous example are

$f_a$ = 6.85 Ghz, $f_m$ = 1.5 Ghz, g = -0.0735

These constants when used in equation 11 yield the curve of Figure 21, illustrating an excellent fit to the experimental data. (Later measurements show that $f_m$ = 1.3 provides a better fit to the VTO used in Model No. 6.) (Note: fm = fa-fb, fa was just estimated and fb is read directly from Figure 21.)

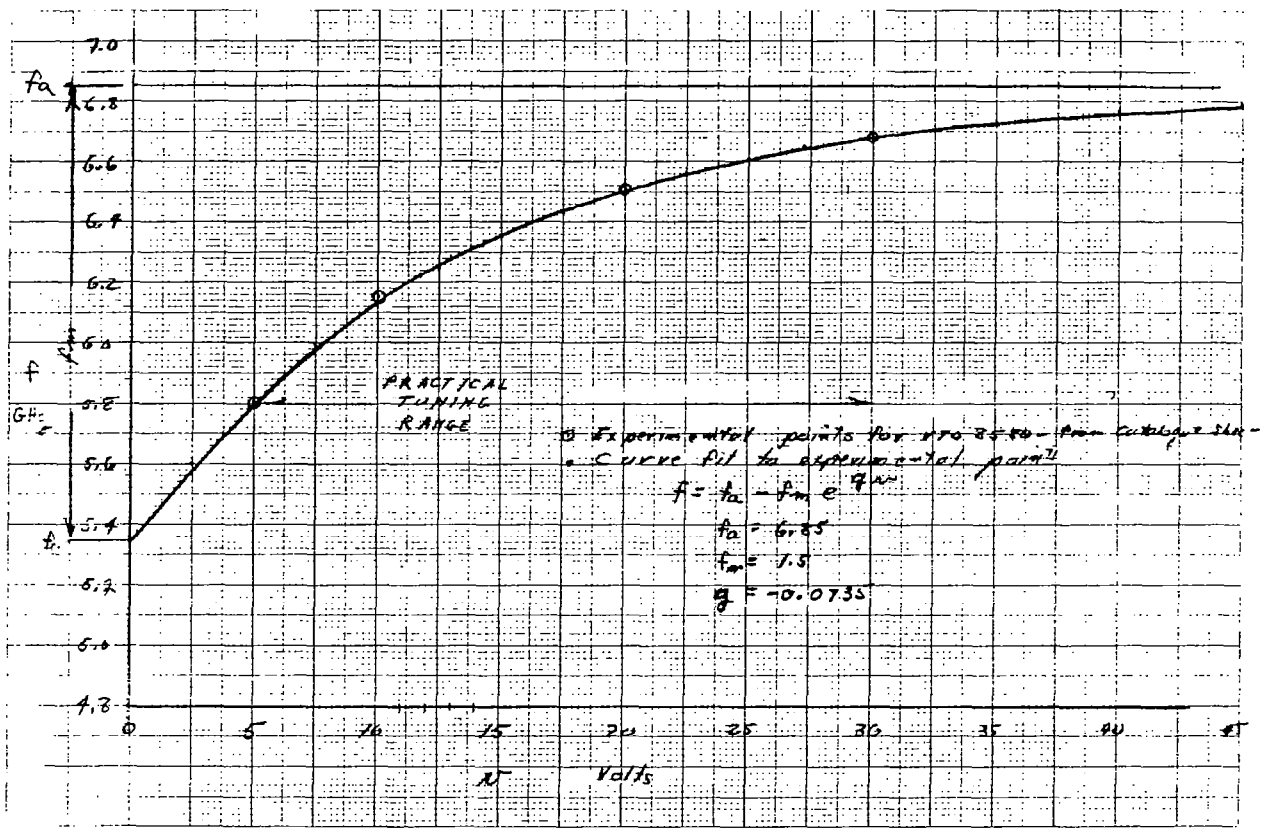


FIGURE 21 - VARACTOR TUNED OSCILLATOR TUNING CURVE

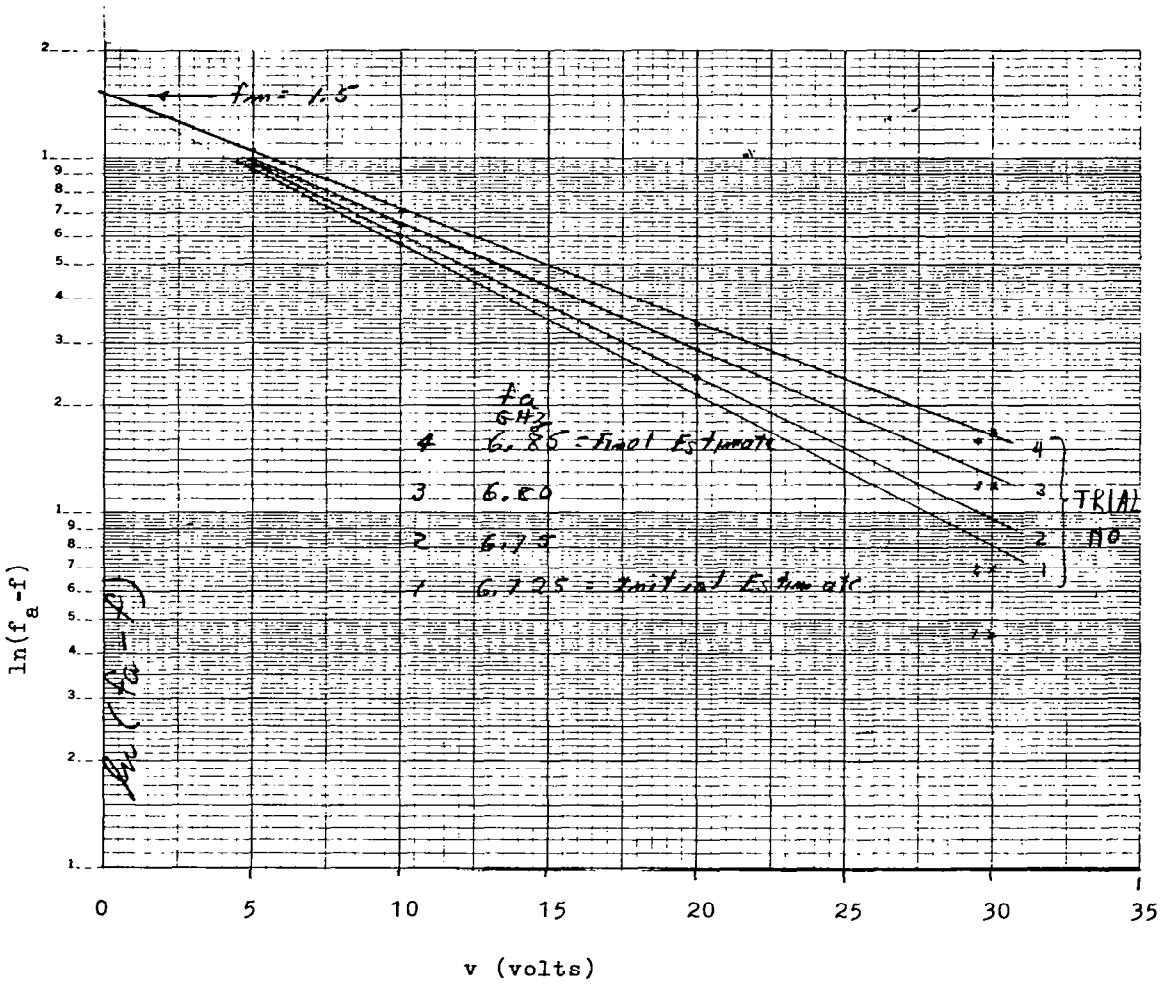


FIGURE 22 - TECHNIQUE TO ESTIMATE fm AND fa FOR A VTO

## 4.0 MEASURED CHANGE IN FREQUENCY (df) WITH CHANGE IN FREQUENCY INDEX (di)

The change in frequency due to the applied frequency index was measured in the following manner

Known thicknesses of polyethelene were applied to the MIAMI transducer and the frequency shift produced was measured in the laboratory at room temperature. Data is presented in Figures 13-16 and summarized in Table 2 and is plotted in Figure 23. Known thicknesses of polyethelene tape were also applied to MIAMI transducer and the change in applied frequency index measured, and are plotted in Figure 24.

From Figure 23 and 24, the change in frequency produced by a change in index is established and is graphed in Figure 25.

The change in frequency due to change in index may also be established from the VTO tuning curve given the relationship between drive voltage and frequency index and the constants of the VTO as presented in Equation 10. Good agreement between eq 10 and Figure 25 is achieved when fm = 1.3, g = 0.035 m = 0.0058 and voo = 11.68 volts.

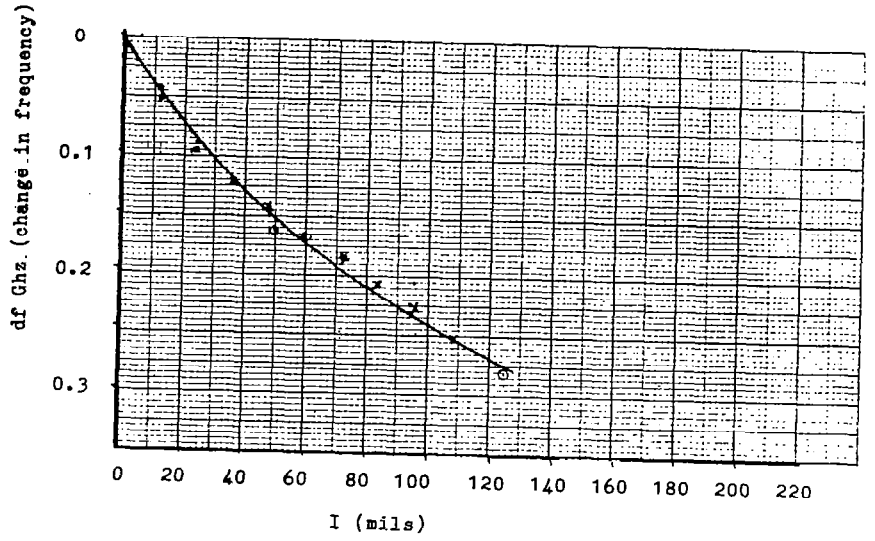


FIGURE 23 - RESONANT FREQUENCY SHIFT (MEASURED) DUE TO LAYERS OF POLYETHELENE ON MIAMI TRANSDUCER

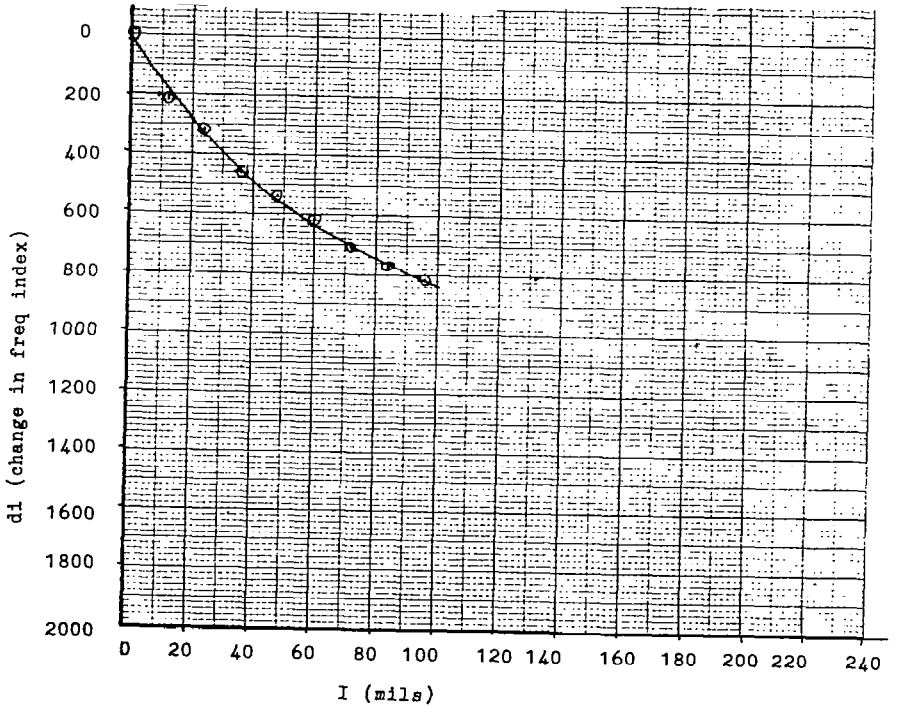


FIGURE 24 - CHANGE IN FREQUENCY INDEX (MEASURED) DUE TO POLYETHELENE ON MIAMI TRANSDUCER

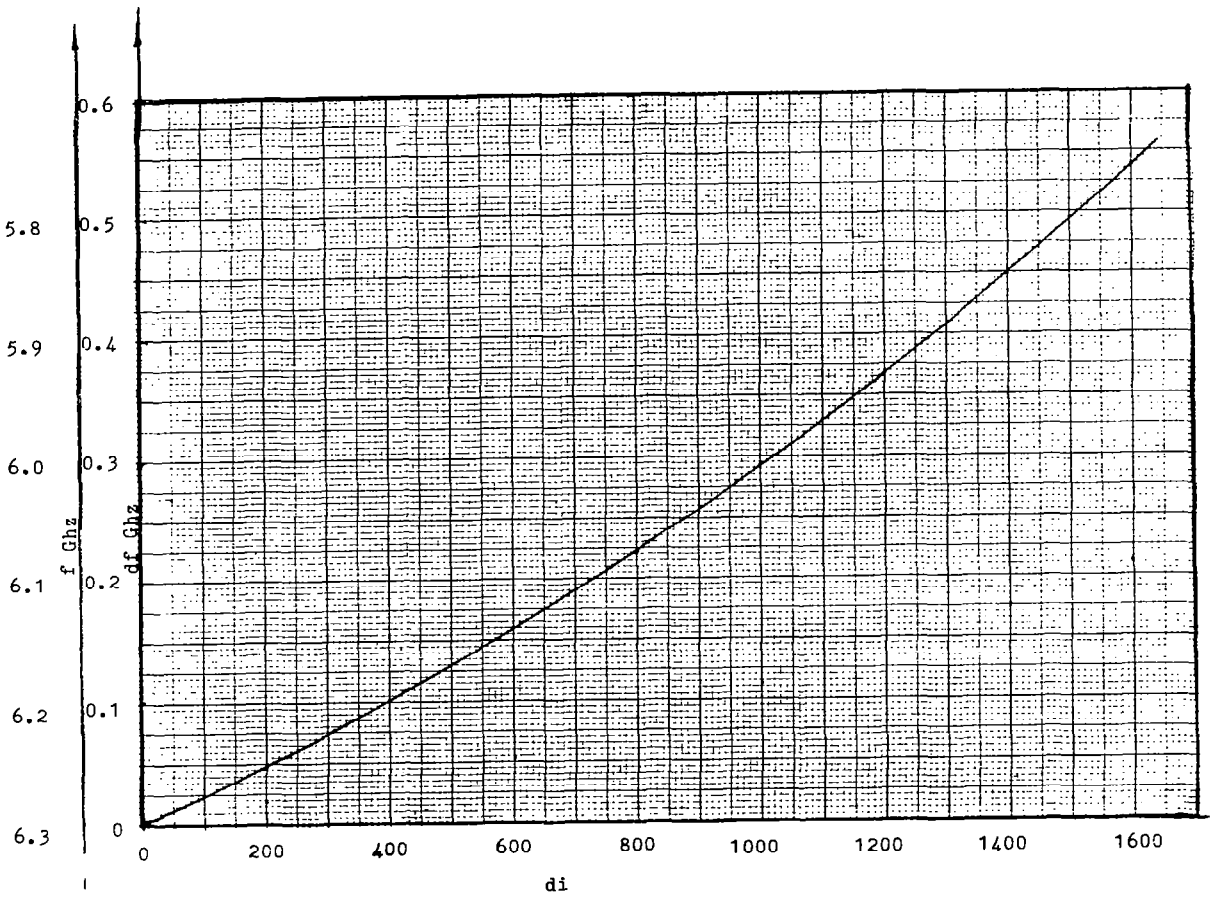


FIGURE 25 - FREQUENCY AND CHANGE IN FREQUENCY AS A FUNCTION OF CHANGE IN FREQUENCY INDEX - MIAMI MODEL NO. 6 FROM JUNE TESTS

## 5.0 EQUIVALENT CIRCUIT THEORY OF MIAMI TRANSDUCER

A physical circuit of the MIAMI transducer appears in Figure 26 with a layer of ice that is smaller than the base dielectric doo. The thickness of the base dielectric doo is designed so that in the absence of ice the surface waveguide between terminals 1 and 2 can support the TE1 mode surface wave and therefore can be considered a "uniform transmission line" of thickness doo. When an ice layer of thickness I, with I always less than doo, is added the modified waveguide between terminals 1 and 2 can still support the TE1 surface wave, however, since the ice layer of thickness I is always less than doo, the ice outside terminals 1 and 2 cannot support the TE1 mode. This ice appears as a waveguide beyond cut-off to the surface waveguide between terminals 1 and 2, and presents an inductive load to the waveguide at terminals 1 and 2 as shown in Figure 26b. Even in the absence of ice, the end plates at terminals 1 and 2 are not perfect short circuits but also present an inductive load to the waveguide. Thus, the inductance shown in Figure 26b has contributions from the end plates as well as the ice layers.

From transmission line considerations (Smith Chart) a short length of transmission line is inductive so that the inductance of Figure 26b may be replaced by two short transmission lines of length $l'$. The waveguide is resonant when the equivalent length of transmission line is equal to an integral number of half guide wavelengths.

The theoretical tuning curve for a polyethelene surface waveguide was derived assuming the inductances presented to the transmission line were fixed. Since these vary also with ice thickness, we should expect the measured tuning curve to deviate somewhat from the theoretical curve.

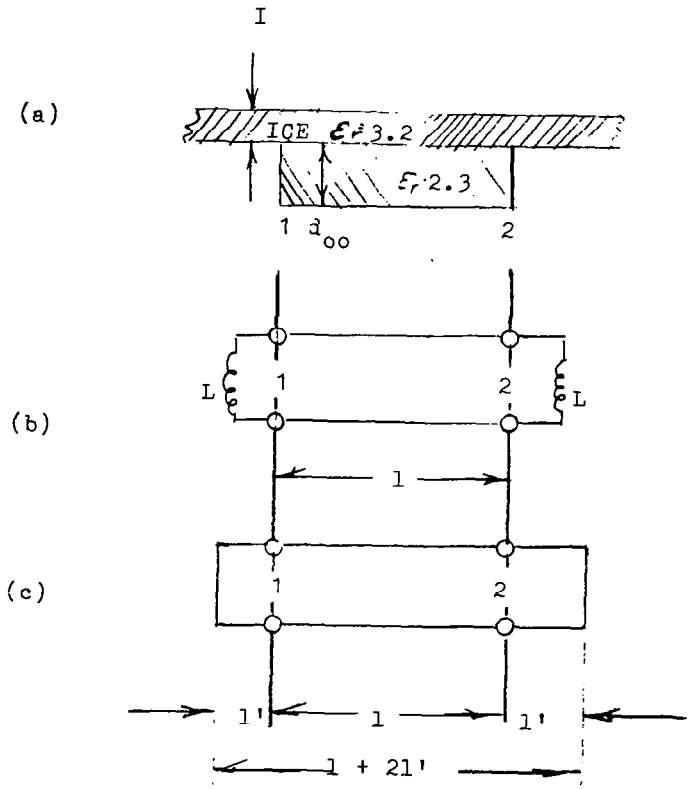


FIGURE 26 - EQUIVALENT CIRCUIT - MIAMI TRANSDUCER

APPENDIX 2 - SYSTEM DOCUMENTATION

## 1.0 THE MICROPROCESSOR

The general structure of the MIAMI, including the microprocessor is shown in Figure 27. In operation, the computer generates a number J which is presented to the DAC (a)1 at its memory location Ø8ffØH. The DAC converts the number to a current that is linearly related to J by $I = K_1 J + K_2$ which ranges between 4 and 20 ma for J = 1 to 2047. This current is then transmitted to the transducer via a long cable where it is impressed across the input resistor of the VTO driver where it is converted into a voltage and is amplified by the VTO to the 0 to 30 volt range for driving the VTO. The VTO in response to the tuning voltage oscillates in the 5.8 to 6.6 Ghz band, its exact frequency being a function of the tuning voltage.

The signal is then passed through the resonant surface waveguide and then detected by the crystal detector resulting in a negative voltage between 0 and -0.5 volts. This voltage is then amplified by the detector amplifier and transmitted via the long cable to the ADC boards in the computer. The returned voltage Aj is presented simultaneously to two ADC converters, one with unity gain and the other with a gain of 3 for use when the signal is weak. After conversion by the ADC's, one or another of the two resulting numbers is read by the computer and represents the response of the resonant surface waveguide (plus its ice load) to the applied VTO frequency f (J).

The computer then emits another value of J and processes the returns, looking for a maximum $A_J$. When a maximum $A_J$ is found, the value of J, which produced it, ML, is the "resonant frequency index." The quiescent frequency $f_{\infty}$ (no ice) produces a frequency index CA or calibration index.* A function if CA-ML = DX is then related to the ice thickness at the transducer.

*As of 9/9/81, if CA=1505, foo=6.29 Ghz, MX=1465

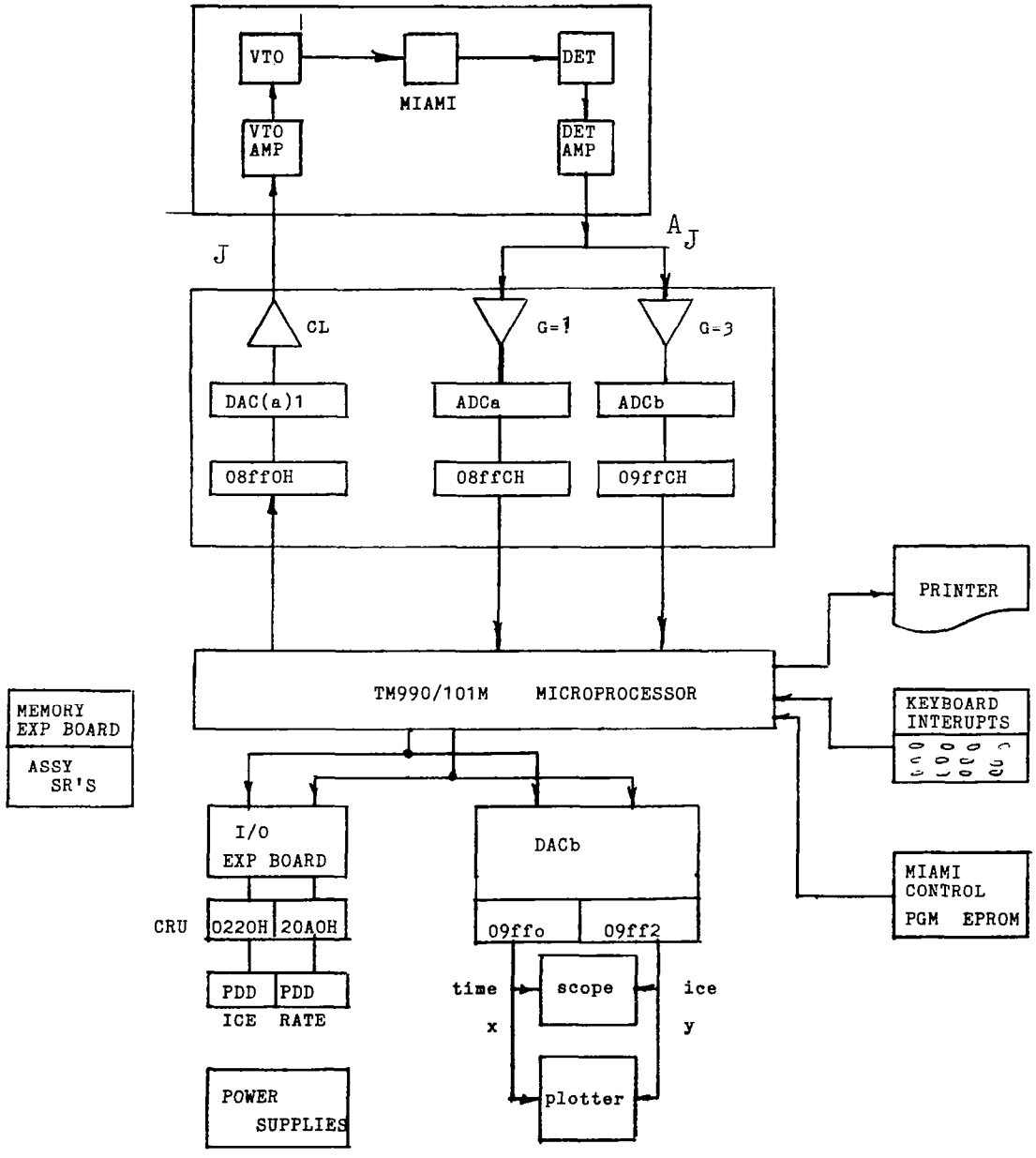


FIGURE 27 - MIAMI SYSTEM STRUCTURE

When ML is found, it is used by the computer to determine the range of values of J to be presented next, J1 to J2, and the process of searching for the peak between J1 and J2 is repeated, J again ranging downward in unit steps from J1 to J2. The sampling rate is 6000 frequencies/sec., every one half second for the first 30 seconds, and every second thereafter. At the completion of a sweep, the latest values of DX, the time of the on-board clock T, and ice thickness $\Theta$, and the amplitude of the peak (number proportional to its voltage) MX, are stored in an array in computer memory. At the same time, one of three possible pairs of values is presented to the oscilloscope and plotter input terminals, and ice thickness and accretion rate are converted to decimal (from the computer's binary) and presented to the two panel digital displays (PDD's).

Data available for online oscilloscope/plotter output are the pairs: (time, $\Theta$), (time, ML), (J, Aj), where the first term appears as the x-coordinate, and second as y. While the oscilloscope and plotter are in general operated in parallel, it is possible to read J, $A_J$, on the oscilloscope while plotting any of the other pairs at the same time.

The program as stored on EPROM does not provide for alternate displays, nor different kinds of plots, outputs are J, $A_J$, during test, MX, ML after calibration and $\Theta$, T after icing starts. For alternative outputs, the program must be read in from cassette tape and proper modifications made in the code. Alternate post-run plots are also coded (but not linked) in the taped program.

Interrupts (to switch functions of the computer) are presented via key strokes on the printer during execution. For calibration of ice thickness as seen by the MIAMI with ice thickness as seen by a transit, a "Mark!" stroke, entered via the keyboard as a CR (carriage return), records the time at which the event

occurred. (See operating instructions.) At the completion of a run, the data stored are printed, and other plots can be made, in pairs, from the set T (time), $\theta$, $\dot{\theta}$, ML, MX, where $\dot{\theta}$ is accretion rate ($d\theta/dt$). Then the data are erased and the program reset for the next run.

The two most frequently used subroutines, "PEAK" (which sweeps the range of frequencies and determines the peak) and "HEXDEC" (which converts binary to decimal for PDD display) are coded in assembly language. The rest of the program is BASIC.

## 1.1 Peak Following Algorithm

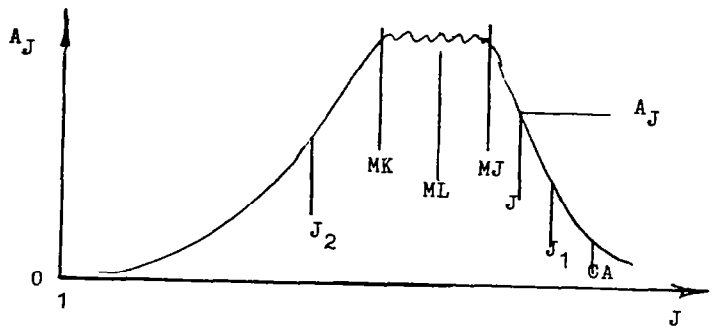


J is decremented from J1 to J2. A is amplitude of return signal.

MX is highest value of A found.

MJ is value of J at which MX is first found.

MK is value of J at which MX is last found. (May be equal to MJ)

ML = (MJ + MK)/2.

CA is ice-free (quiescent resonant frequency) index.

Initial value of J1 = CA + 32, J2 = CA -32.

New values of J1 and J2, after sweep is completed,

are J1 = ML-48, J2 = ML+48, unless

MK-J2 $<$ 3 in which case J1 = J2 + 16, J2 = J1-96

or

J1 - ML $<$ 3 in which case J2 = J1 - 16, J1 = J2 +96

or

ML $>$ CA in which case J1 = CA +8, J2 = CA - 88

or

MX $<$ 500 or OS $\geq$ 8 in which case J1 = CA, J2 = 1

where OS is amplification flag. If OS = 8, 9,10 or 11 then A is amplified by 3 and sweep covers entire range.

If MX $<$ 500 and OS $<$ 8 then OS = OS + 8

If MX $>$ 2000 and OS $>$ 7 then OS = OS - 8

This provides 'hysteresis' to prevent oscillation. During test (before calibration) J1 = 2000, J2 = 1

## 1.2 Averaging Subroutine

During calibration , to the nearest integer

$$CA = 1/30 \sum_{I=1}^{30} ML_I$$

The ice trigger is

$$IT = CA - 2*MIN(ML_I)$$

When waiting for ice if in any sweep

$$CA-ML > IT$$

the assumption is that icing has begun.

Ice thickness smoothed TT and accretion rate TK are determined from the six most recent readings of TH=f(CA-ML) and fitted by a least squares straight line.

## 2.0 THE COMPUTER PROGRAM

### 2.1 Flow Charts

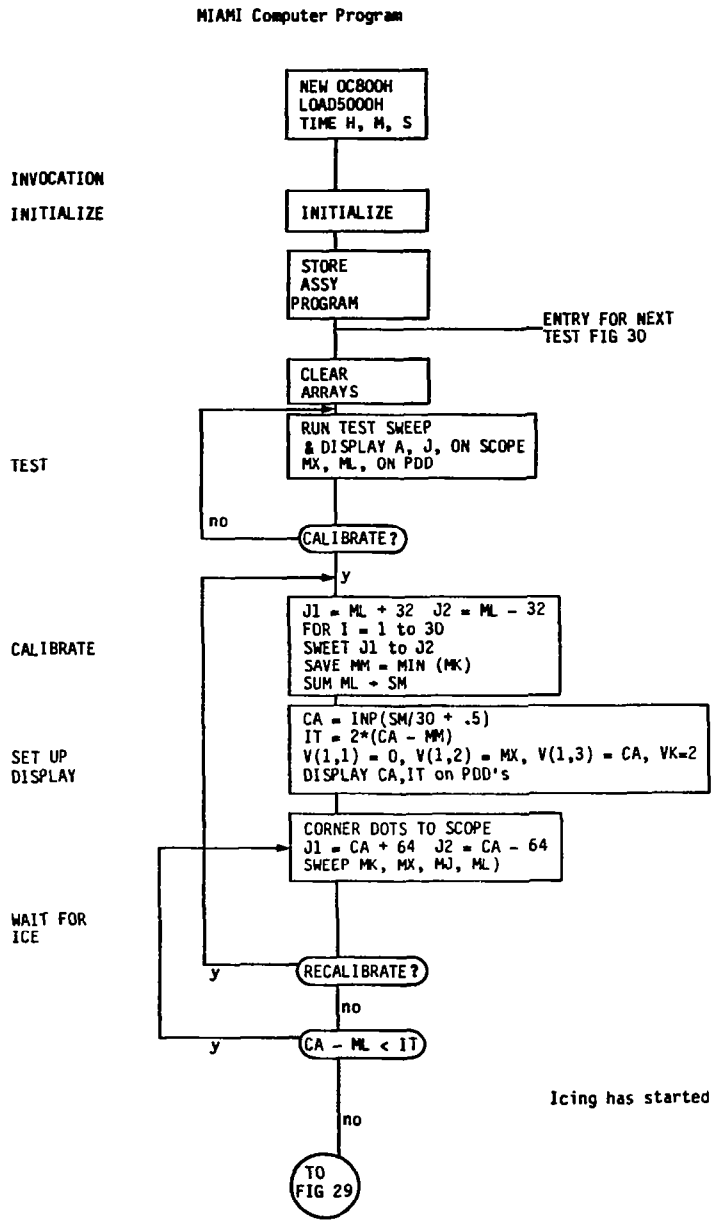


FIGURE 28 - MIAMI COMPUTER FLOW CHART

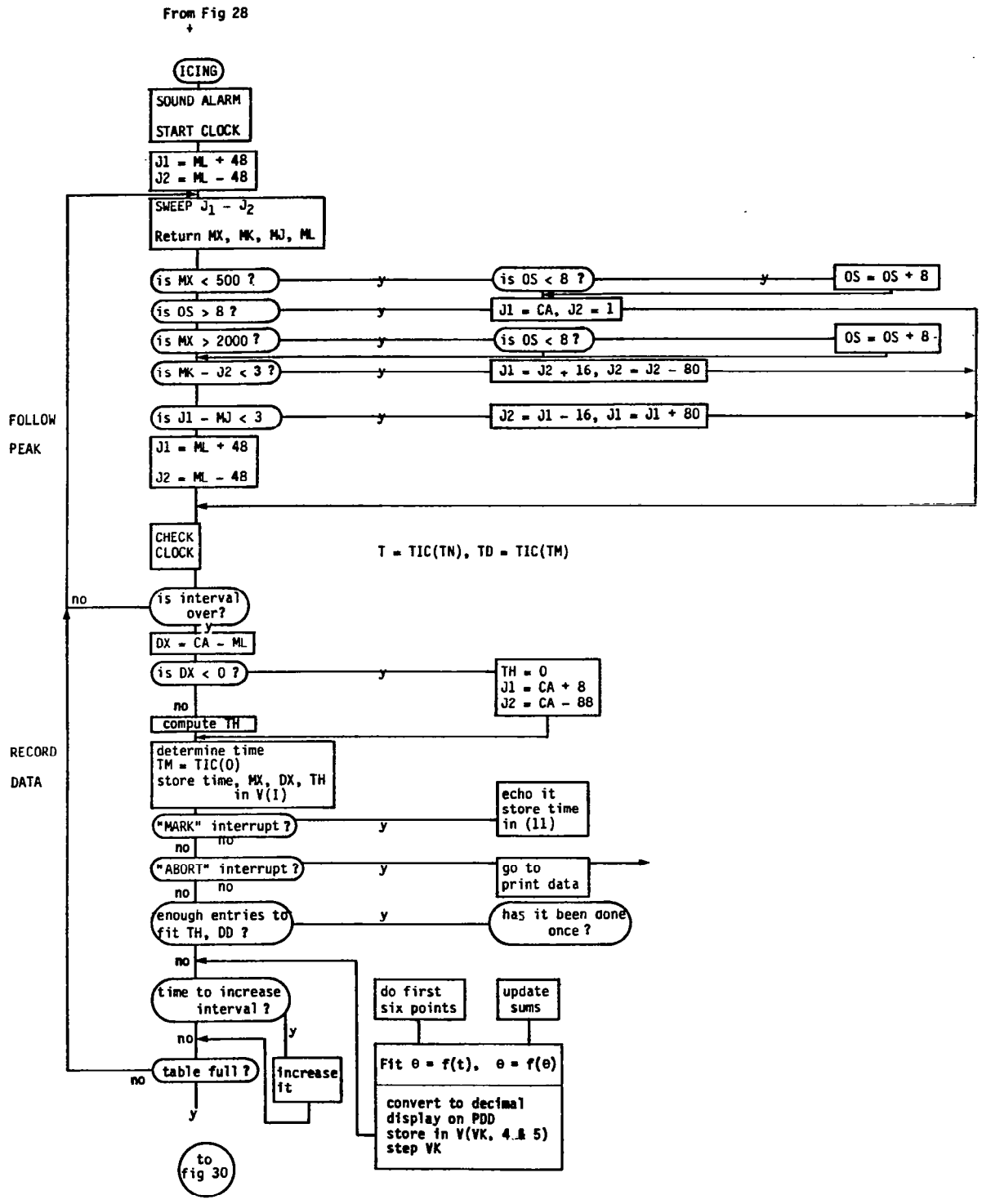


FIGURE 29 - MIAMI COMPUTER FLOW CHART

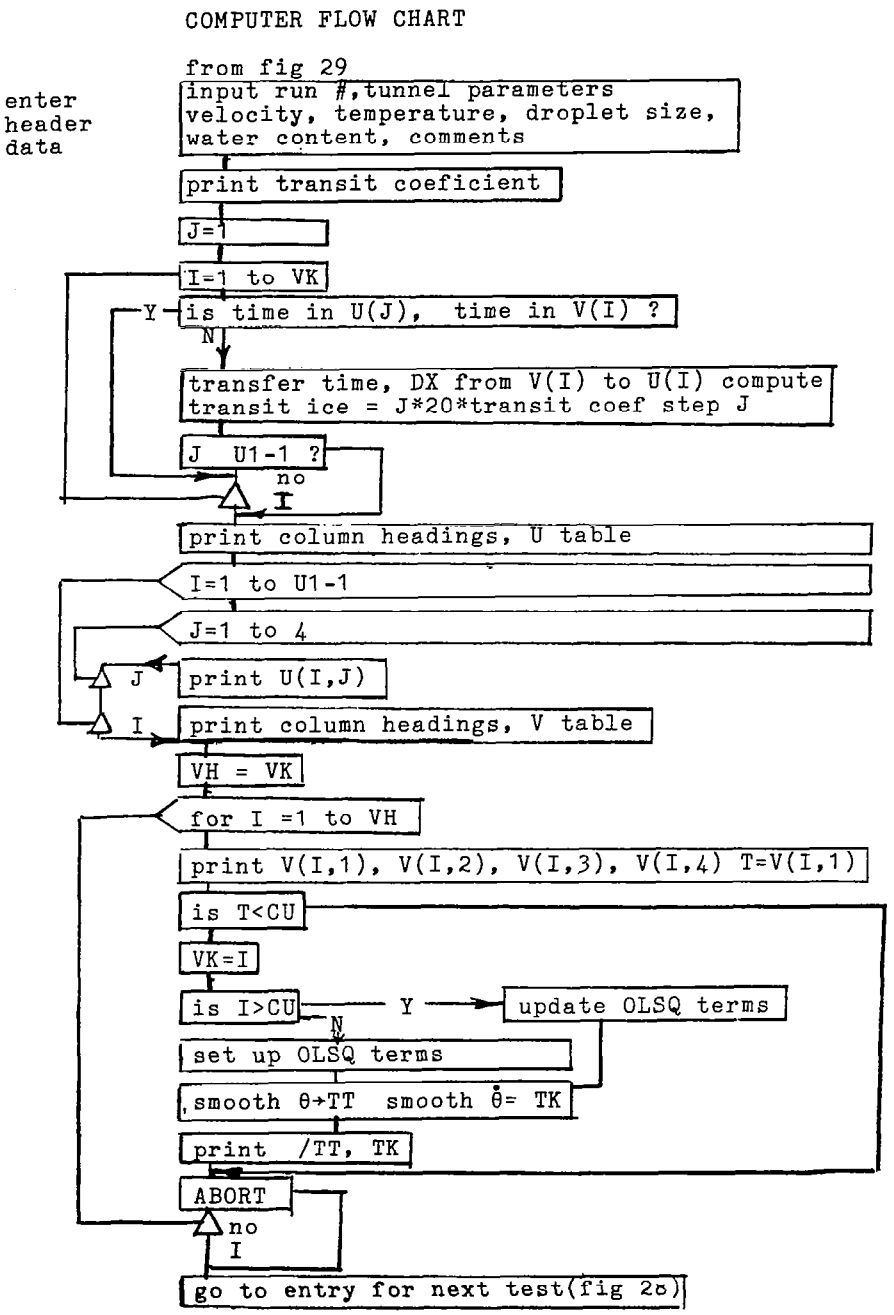


FIGURE 30-MIAMI COMPUTER FLOW CHART

COMPUTER FLOW CHART

ASSEMBLY PROGRAM "PEAK"

```
            set up working storage
            find and store return address
            clear status words, both boards
            select input channel, both boards

            move J1 to J
            load -999 into  A   (R5)
            load -1000 into MX (R6)
A4          move J → DAC A output (next cycle)
            start conversion both boards this cycle
            compare last value of A with MX
            if A < MX* go to A1
            if A =mx go to A2
            move A to MX
            move J to MJ
A2          move J to MK
A1          compare OS flag with 8 bit (gain)
            if low gain go to A5
A3          if conversion is not complete, go to A3 *
            move input data ('A') to high gain
            jump to A7
A5          if conversion is not complete, go to A5 *
            move input data ('A') to low gain board
A6          if OS<>1 (display A,J) go to A7
A7          decrement J output A,J to ADC
            if J < J2 go to A4
            calculate (MJ+MK)/2 = ML
            return
```

*( spin here until conversion is complete)

FIGURE 31

## 2.2 Main Control Program, Definitions

| | |
|---|---|
| T(3) | storage for time |
| V(241,4) | data table for time, MX, TH, DX |
| U(30, 4) | transit reading tabletime, DX, TRANSIT ICE, MIAMI ICE |
| C2,C3,C4, C5, | coefficients of fifth order polynomial $\theta = \sum_{i=1}^{5} C_i DX^i$ |
| $B | token for beeper |
| CA | calibration index nominally 1770 |
| ML | resonant frequency index |
| DX | CA-ML |
| CU | row in v table at which to start smoothing |
| U | memory address (hex) of ADC(1) data block |
| V | memory address (hex) of ADC(2) data block |
| W | memory address (hex) of workspace for assembly 'PEAK' |
| MX | maximum value of $A_J$ |
| MK | last (lowest) value of J for which A=MX |
| MJ | first (highest) value of j for which A=MX |
| MWD(W+6) | increment between steps in "PEAK" subroutine |
| TT | smoothed ice thickness |
| DEF(DX) | DXd(C2+DX(C3+DX(C4+DX(C5+DX*C6)))) |
| U1 | row index of U table |
| U2 | flag, U table overflow |
| VK | row index of V table |
| S | step in J same as MWD(W+6) |
| J1 | initial (start) value of sweep frequency index |
| J2 | final (end) value of sweep frequency index |
| OS | amplification and display flag<br>8,0 no display<br>9,1 amplitude j<br>AH peak amplitude J<br>CH ice thickness, time<br>if OS > 7 amplification is 3<br>if os < 8 amplification is 1 |

truth table

| OS | 0-500 | 500-2000 | 2000 |
|---|---|---|---|
| < 8 | OS → 8 | - | - |
| > 7 | - | - | OS → < 8 |

| | |
|---|---|
| Z1,Z2 | arguments for 'HEXDEC" |
| A | keyboard interrupt character |
| SM | sum of readings of MK during calibration |
| MM | minimum reading of MK during calibration |

## 2.2 Definitions (cont'd)

| | |
|---|---|
| CT | if CU=13, storage interval is 13/25 seconds<br>if CU=25, storage interval is 25/25 seconds |
| IT | ice trigger |
| TN | time since clock started, equals moment ice starts to form |
| TM | equates TN, first storage interval in 25ths of a second (1 tick = 40 ms.) |
| T | time since start of icing |
| TD | time since last storage |
| TH | ice thickness |
| TM | time now defined in 1050 |
| line1075 | ASCII CHAR<br>13 carriage return<br>65 A<br>66 B<br>67 C<br>68 D<br>69 E |
| $A | input string, printed, not saved |
| M | transit coefficient. Since this number (.93) is stored on EPROM if a different value is used U table values of observed ice must be adjusted manually |
| TT | smoothed value of ice thickness |
| TK | smoothed accretion |
| S1,S2,S3, S4,S5 | terms in least squares fit |
| DN | denominator, if zero start at next point |
| M1 | accretion rate mils/second |
| A1 | intercept |

### SYSTEM DESIGN NOTATION

| | |
|---|---|
| J | index number $0<J<2048$ |
| K1,K2 | constants: local to expression |
| $A_J$ | amplitude of return signal before ADC |
| f(J) | frequency generated by VTO |
| ML | ML=(MJ+MK)/2 |
| $f_{oo}$ | quiescent resonant frequency |
| CA | quiescent frequency index (calibration value) |
| DX | CA-ML |
| J1 | first value of J presented during sweep |
| J2 | last value of J presented during sweep<br>$J1>J2$ |
| MX | amplitude of peak (maximum value of A found) |
| T,t | time in seconds |
| CR | carriage return |
| Θ,TH | ice thickness |
| TT | ice thickness smoothed |

## 2.3 Program Listing

```
SAVE 2
NEW
TM990 BASIC REV D.1.10
*READY
LOAD 05000H
LIS
 10  REM    ****MIAMI CONTROL PROGRAM****
 11  REM      IDEAL RESEARCH, INC., ROCKVILLE, MD.
 12  REM        AUTHOR: JAMES K. ROCKS
 13  REM     DEVELOPED UNDER NASA CONTRACT, 1981
 14  REM            ALL RIGHTS RESERVED
 20  DIM T[3],V[241,4],U[30,4]
 25  TIME 0,0,0
 30  TIME $T[0]
 40  C2=0.0426936341:: C3=-0.00009568097:: C4=3.50247865E-07
 42  C5=-3.49928882E-10:: C6=1.25803687E-13:: $B=%7%0:: BX=0:: CU=7
 44  CA=1770:: U=08FF0H:: V=09FF0H:: W=0C700H:: MK=0:: MJ=0:: ML=0
 46  MWD[W+6]=-1:: TT=0
 50  DEF FND[@]=[*(C2+[*(C3+[*(C4+[*(C5+[*C6)))
 405  DATA 0C700H,0C008H,0420H,0C000H
 410  DATA 0200H,016H,0A00DH,0C390H,04E0H,08FF4H
 420  DATA 04E0H,09FF4H,0200H,01H,0C800H,08FF8H,0C800H,09FF8H,0C001H,0205H
 430  DATA 0FC19H,0206H,0FC18H,0C800H,08FF0H,0720H,08FFAH,0720H,09FFAH,08185H
 440  DATA 01104H,01302H,0C185H,0C1C0H,0C200H,02120H,0C084H,01606H,0560H
 450  DATA 09FFCH,011FDH,0C160H,09FFEH,01005H,0560H,08FFCH,011FDH,0C160H,08FFEH
 460  DATA 02120H,0C07EH,01604H,0C805H,09FF2H,0C800H,09FF0H,0A003H,08080H
 470  DATA 015DCH,0C247H,0A248H,0819H,0380H,01H,02H,04H,08H
 500  FOR I=0C000H TO 0C084H STEP 2:: READ A:: MWD[I]=A:: NEXT I
 510  DATA 0C720H,0C108H,0420H,0C100H,0200H,016H,0A00DH,0C390H,0C0A0H
 512  DATA 0C7FAH,04C0H,0204H,04H,0205H,0AH,0B40H,0C082H,0130CH
 514  DATA 0C0C2H,04C2H,03C85H,0E003H,0604H,016F7H,0B40H,0C042H,01000H
 516  DATA 01000H,01000H,0380H,0B40H,0604H,016FDH,010F7H
 520  FOR I=0C100H TO 0C142H STEP 2:: READ A:: MWD[I]=A:: NEXT I
 600  FOR I=1 TO 240:: FOR J=1 TO 4:: V[I,J]=0:: NEXT J:: NEXT I
 610  FOR I=1 TO 30:: FOR J=1 TO 4:: U[I,J]=0:: NEXT J:: NEXT I
 620  U1=1:: U2=0:: VK=1
 700  S=-1:: J1=2000:: J2=1:: DS=1
 710  GOSUB 5010
 730  Z1=MX:: Z2=0220H:: GOSUB 4000:: Z1=ML:: Z2=02A0H:: GOSUB 4000
 750  A=NKY[0]:: IF A<>67 THEN GOTO 710
 810  DS=1:: SM=0:: MM=2000:: CT=13
 820  J1=ML+32:: J2=ML-32
 830  FOR I=1 TO 30:: GOSUB 5010:: SM=SM+ML
 840   IF MK<MM THEN MM=MK
 850  NEXT I:: CA=INP[SM/30+0.5]:: IT=2*(CA-MM)
 860  V[1,1]=0:: V[1,2]=MX:: V[1,3]=CA:: V[1,4]=0:: VK=2
 905  Z1=CA:: Z2=0220H:: GOSUB 4000:: Z1=IT:: Z2=02A0H:: GOSUB 4000
 910  MWD[09FF0H]=2000:: MWD[09FF2H]=2000
 915  DS=4:: MWD[09FF0H]=0:: MWD[09FF2H]=0
 920  J1=CA+64:: J2=CA-64
 930  GOSUB 5010
 935  A=NKY[0]:: IF A=67 THEN GOTO 810
 940  IF CA-ML<IT THEN GOTO 910
 960  DS=4:: TN=TIC[0]:: PRINT $B:: TM=TN
 970  J2=ML-48:: J1=ML+48
 980  GOSUB 5010
 990  IF DS<8 AND MX>500 THEN GOTO 1010
 995  IF DS>7 AND MX<2000 THEN GOTO 1007
 1000  IF DS<8 AND MX<500 THEN DS=DS+8:: GOTO 1007
 1005  IF DS>7 AND MX>2000 THEN DS=DS-8:: GOTO 1010
 1007  J1=CA:: J2=1:: GOTO 1030
 1010  IF ABS[MK-J2]<3 THEN J1=J2+16:: J2=J2-80:: GOTO 1030
 1015  IF ABS[J1-MJ]<3 THEN J2=J1-16:: J1=J1+80:: GOTO 1030
 1017  J1=ML+48:: J2=ML-48
 1030  T=TIC[TN]:: TD=TIC[TM]
 1040  IF TD<CT THEN GOTO 980
```

```
1045  DX=CA-ML:: IF DX<0 THEN TH=0:: J1=CA+8:: J2=CA-88
1046  TH=FND[DX]
1050  TM=TIC[0]:: V[VK,1]=T/25:: V[VK,2]=MX:: V[VK,3]=CA-ML:: V[VK,4]=TH
1075  A=NKY[0]:: IF A<>13 THEN GOTO 1082
1080  PRINT ".":: U[U1,1]=T+0.04:: U1=U1+1:: IF U1>30 THEN U1=30:: U2=U2+1
1082  IF A=66 THEN GOTO 1500
1084  IF VK>CU THEN GOSUB 7000
1086  IF VK=CU THEN GOSUB 7200
1090  VK=VK+1
1100  IF VK<60 THEN GOTO 980
1110  CT=25
1120  IF VK<241 THEN GOTO 980
1500  INPUT "RUN NUMBER: "}$A:: INPUT "TUNNEL PRAMS: VEL="}$A}
1520  INPUT "  TEMP(F)="}$A}:: INPUT "  DROPLET SIZE="}$A}
1530  INPUT "  WATER CONTENT="}$A
1540  INPUT "COMMENTS: "}$A
1545  M=0.93
1550  PRINT "TRANSIT COEFFICIENT: "}M:: PRINT :: PRINT
1840  J=1
1850  FOR I=1 TO VK
1860   IF U[J,1]>V[I,1] THEN GOTO 1890
1870   U[J,4]=V[I,4]:: U[J,2]=V[I,3]:: U[J,3]=M*J*20:: J=J+1
1880   IF J>=U1 THEN GOTO 1900
1890  NEXT I
1900  PRINT " TIME      D-INDEX     TRANSIT ICE  MIAMI ICE"
1910  FOR I=1 TO U1:: FOR J=1 TO 4:: PRINT #"SSSS.99      "U[I,J]}
1920   NEXT J:: PRINT :: NEXT I
1930  PRINT "TIME","RESONANT","FREQUENCY","THICKNESS","ACCRETION"
1941  PRINT "SECS","AMPLITUDE","  SHIFT","MILS OF ICE","RATE,MILS/MIN"
1945  VH=VK
1950  FOR I=1 TO VH:: PRINT V[I,1],V[I,2],V[I,3],
1955   PRINT #"SSSSS.9"V[I,4]}
1956   T=V[I,1]
1960   IF I<CU THEN PRINT :: GOTO 1966
1962   VK=I:: IF I>CU THEN GOSUB 7000:: GOTO 1965
1964   IF I=CU THEN GOSUB 7200
1965   PRINT "/"}#"SSS.99  "TT}"     "}#"SSS.99"TK
1966   A=NKY[0]:: IF A=66 THEN GOTO 1972
1970  NEXT I
1972  PRINT :: PRINT
1975  VK=VH
1980  PRINT "ENTER A FOR NEXT TEST,D TO REDO REPORT, E TO REDO REPORT WITHOUT H
DR:"
1981  PRINT :: PRINT :: PRINT :: PRINT :: PRINT
1982  A=NKY[0]:: IF A=0 THEN GOTO 1982
1985  IF A<65 OR A>69 THEN GOTO 1980
1990  ON A-64 THEN GOTO 600,1980,1980,1500,1840
4000  MWD[0C7FAH]=Z1:: CALL "HEXDEC",0C104H:: BASE Z2:: CRF[0]=MWD[0C720H]
4010  RETURN
5010  MWD[W+2]=J1:: MWD[W+4]=J2:: MWD[W+8]=03
5020  CALL "PEAK",0C004H
5030  MX=MWD[W+12]:: ML=MWD[W+18]:: MJ=MWD[W+14]:: MK=MWD[W+16]
5040  RETURN
7000  S1=S1+V[VK,1]*V[VK,4]-V[VK-6,1]*V[VK-6,4]
7010  S2=S2+V[VK,1]-V[VK-6,1]:: S3=S3+V[VK,4]-V[VK-6,4]
7020  S4=S4+V[VK,1]*V[VK,1]-V[VK-6,1]*V[VK-6,1]
7050  S5=S2*S2:: DN=6*S4-S5:: IF DN=0 THEN CU=CU+1:: RETURN
7070  M1=(6*S1-S2*S3)/DN:: TK=M1*60
7080  A1=(S3*S4-S1*S2)/DN:: TT=V[VK,1]*M1+A1
7110  Z1=TT:: Z2=0220H:: GOSUB 4000:: Z1=TK:: Z2=02A0H:: GOSUB 4000
7130  MWD[09FF0H]=0.3*T+300:: MWD[09FF2H]=TT*8:: RETURN
7200  S1=0:: S2=0:: S3=0:: S4=0:: S5=0
7210  FOR IS=VK-7 TO VK:: S1=S1+V[IS,1]*V[IS,4]
7220   S2=S2+V[IS,1]:: S3=S3+V[IS,4]:: S4=S4+V[IS,1]*V[IS,1]
7230  NEXT IS
7240  GOTO 7050
```

## 3.0 COMPUTER HARDWARE

The computer is a Texas Instrument TMS990/101M micro-computer using the TMS9900 16-bit microprocessor and 16K bytes (of 8 bits) of RAM. The system presently includes:

a. TM 990/101M. The 101-M board (slot 1) holds the TI9900 microprocessor, a 9901 CRU processor, 4K of EPROM (the BASIC interpreter) 2K bytes of RAM and various drivers and buffers. The jumper settings are E1-2, 4-5, 7-8, 9-10, 13-14, 16-17, 18-19, 22-23, 24-25, 26-27, 28-29, 31-32, 33-34, (these four pairs designate type 2716 EPROMs), 39-40, 54-55. Dip switch is irrelevant since there is only a single user. The two 47 uf capacitors (C8 and C23) debounce the switches. Memory on this board maps EPROM from ØØØØ to 1FFFH, and RAM from ØFØØØH to ØFFFFH. The KSR terminal is connected by cable to P2.

b. TM 990/201-42 (Slot 2) memory expansion board has 4K RAM and 8K EPROM of which 2K holds the MIAMI program and 2K a duplicate. The on-board dip-switch is set to 1-0-0-1-0-1-1-0 to map EPROM onto addresses 2000H to 5FFF and RAM onto addresses 0C000H to 0DFFFH. Both J1 and J2 are set to "slow".

c. TM 990/302 software development board (slot 3), with 4K EPROM holds the development software on EPROM and provides 2K RAM. The EPROM is disabled when the system is in use. It is used for assembly language programming, writing EPROMs and the like. The dip switch is set 1-on, 2-off, 3-off to map RAM to addresses ØEØØØH to ØEFFFH. Rocker switch is depressed on the side corresponding to the word. Jumper settings are E1-E2, E5-E6. The jumper table is standard. The cassette recorders are attached to P-2. P-3 holds the EPROM "personality" module when "burning" EPROMs.

d. TM 990/310 input/output expansion board (slot 4), provides three identical 9901-driven parallel I/O ports (40-pin edge connectors.) Two, P2 and P3, are dedicated to driving the panel digital displays and one is reserved for future development of interrupts, and for digital signals out, e.g., turn on de-icers. The dip switch is set to On-On-On-On which establishes the CRU address of P2 as 0200H, P3 as 280H, and P4 as 0300H. P2 delivers the ice thickness number to the lefthand PDD, while P3 delivers accretion rate, each through 40-wire ribbon cables.

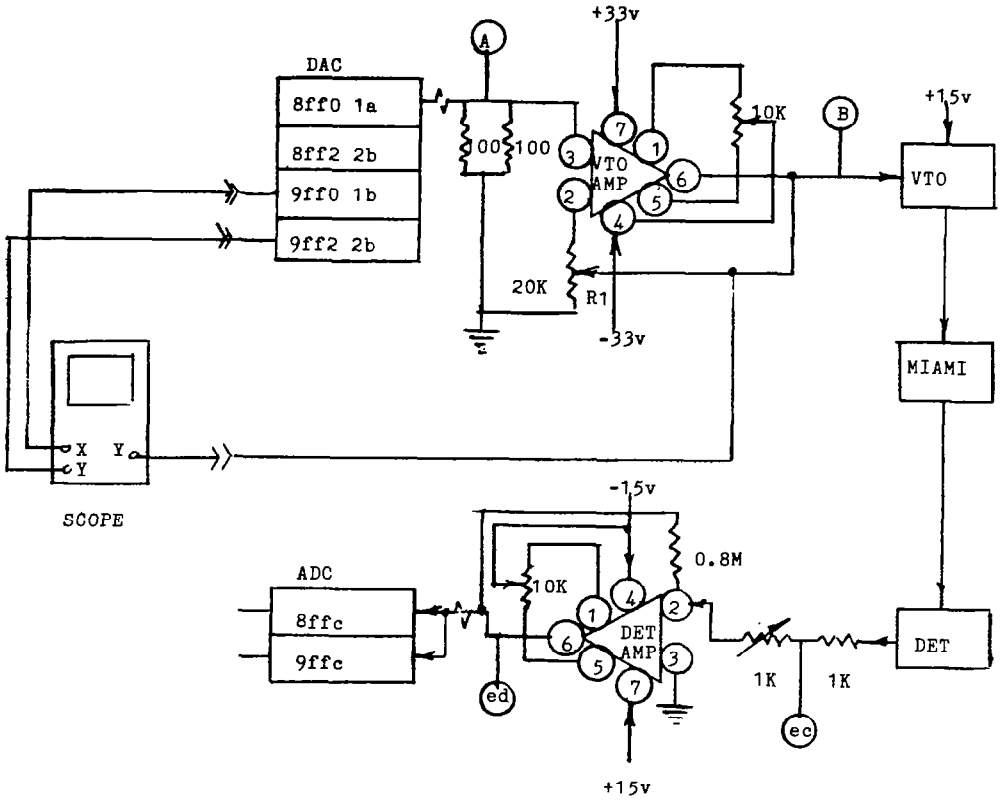


FIGURE 32 - SCHEMATIC MIAMI TRANSDUCER

e. Two Analog Devices 1241-R Analog to Digital converters are in slots 7 and 8. These boards convert digital data to analog voltages or currents for transmission of the frequency index to the MIAMI, and signals to external displays (scope or plotter) and accept the MIAMI response voltage and convert it to a number. The upper board provides a gain of 1, and the lower board a gain of 3. The input signal is delivered to each in parallel and depending on its strength the converted number is read from board 1 or 2 (See program.) Each board is jumpered to appear as an unoccupied block of 16 bytes of main memory of the 101M. Board A has its block beginning at memory address 8ffo, while board B's block is at 9ffo. (Zeros are strapped on the tables where X1 is the high order 4 bits and the low order 4 bits are always zero.) Each board has 2 DAC outputs, each available as both current and voltage and 32 single-ended analog inputs. Connector wiring is given in the following table followed by a table of measured voltages at various points in the transducer.

Cable to MIAMI transducer

| Pin | |
|---|---|
| A | |
| B | i (current loop voltage to MIAMI) (gray ribbon) |
| C | + 15 V (green) |
| D | - 33 V (red) |
| E | |
| F | |
| G | |
| H | +15 V (white) |
| K | GND (black, (ribbon) |
| L | +33 V (blue) |
| M | Ai (voltage) from detector amplifier to ADC input) (ribbon) |
| N | GND |

---

Distribution of cable at MIAMI

Component side,
+15, -15, $A_i$ (out), i (in) +33, GAD, -33

## 4.0 MIAMI OPERATING INSTRUCTIONS

1. After installing the transducer, connect the transducer cable, oscilloscope cables (top to 'x', bottom to 'y',) and ground wire to scope, plug in MIAMI, terminal, scope and connect printer cable to printer.

2. Press latching off/on button on MIAMI power supply. Button should show red light.

3. Press CR on printer, which will type banner message, and "ready".

4. Type NEW ØC8ØØH. Banner will print again.

5. Type LOAD 4ØØØH.

6. Type RUN. MIAMI is now operating. Printed matter should be as follows:

```
TM990 BASIC REV D.1.10
*READY
NEW 0C800H
TM990 BASIC REV D.1.10
*READY
LOAD 4000H
RUN
```

7. Computer now initializes itself and when ready, sends the characteristic resonant sweep to the oscilloscope. Adjust scope to place peak in upper right hand corner and left tail at left lower corner. During this time, digital displays on panel (PDD) will show, left to right, peak amplitude and location of peak, as number of counts. Ignore the decimal points. With no protective layer, left should read about 1949 and right, about 1875. With 25 mils of plastic, counts will be about 1423, 1550. Numbers may jitter in the least significant digit. This is due to inherent noise in the system, and not important. This completes the test of the system.

8. When satisfied with the display, type C (CR), for "calibrate". Displays will read zero. Scope will show a bright

peak at top of curve for a moment, then four dots, one in each corner of the raster. These dots locate the corners of the ice thickness graph which will be generated on the scope as the test progresses. Time from 0 to 240 seconds progresses from left to right across the scope. Ice thickness, in mils, from 0 to 200 progresses from bottom to top. Adjust the scope as required. Then erase the display. The dots will return. System is now ready and waiting for ice. As ice accumulates, its thickness as a function of time will be displayed as a diagonal line on the scope.

9. When about 2 mils of ice have accumulated on the transducer, the beeper will sound and readings of ice thickness will be begun by the computer and stored. Begin transit readings at the same time. Observer should set transit 20 grads ahead of the ice, call out "Mark!" as visible edge of ice passes the transit graticule and then move the graticule another 20 grads. At the same time, the MIAMI operator should press CR on the terminal. Computer will note and store the time at which this occurred for later conversion to ice thickness as a function of number of marks observed. When CR is entered, printer will echo (print) a ".".

10. The program will run for about 210 seconds, recording two measurements each second for the first 30 seconds, then one measurement per second, until 240 measurements have been made or the run is aborted. The run may be aborted by typing "B" any time after it has started. The program jumps to the Report Section upon entry of "B" or when 240 readings have been made.

11. The terminal will ask for Run number, Tunnel parameters (velocity, temperature, droplet size, water content), comments or additional data, and will print the transit calibration coefficient. This number is the number of mils of ice thickness represented by 20 grads on the transit, and should be predetermined as part of the transit calibration procedure.

12. The printer will then output a table giving TIME, in seconds, at which transit reading was noted, D INDEX, a number proportional to shift of resonant frequency from the calibration (zero ice) frequency, TRANSIT ICE thickness as determined from elapsed time and calibration coefficient, and MIAMI ICE thickness, in mils as computed from D-INDEX. If more than 30 "MARK" entries are made, the last entry is repeatedly over-written by its sucessors.

13. All of the data (up to 240 lines) accumulated during the run is now printed. The columns give time of reading, in seconds, resonant amplitude, a number proportional to the power generated by the MIAMI for given ice thickness at resonance; frequency shift, the same number as shown in the previous table list for every entry; thickness of ice in mils as computed by MIAMI; and accretion rate in mils per minute.* Accretion rate is the slope of a least square fit to ice thickness over the last 6 readings, times 60. No calculation of accretion rate is made during the first 5 seconds. The right hand PDD (accretion rate) does not give negative rates (shedding). If the rate is negative, the number appearing (which will contain blanks) is meaningless. The printout may be terminated by typing a "B" (abort) while the listing is being made. The line being printed will be completed, then the printer will space four lines and ask for the operator's next choice, which can be "A" for the next test, in which case memory is zeroed and program returns to Step 11 above; "D" to reprint the report in its entirety; or "E" to reprint the report without header data.

14. To terminate the session, simply turn off the computer, the printer and oscilloscope.

---

* The first row gives in DX the calibration number (DX for foo), all the other numbers in this column are this number less observed DX, thus being proportional to shift in frequency.

| 1. Report No. | 2. Government Accession No. | 3. Recipient's Catalog No. |
|---|---|---|
| NASA CR-3598 | | |

| 4. Title and Subtitle | 5. Report Date |
|---|---|
| DEVELOPMENT AND TEST OF A MICROWAVE ICE ACCRETION MEASUREMENT INSTRUMENT (MIAMI) | November 1982 |
| | 6. Performing Organization Code |
| 7. Author(s) | 8. Performing Organization Report No. |
| Bertram Magenheim and James K. Rocks | BATT-92880 |
| | 10. Work Unit No. |
| 9. Performing Organization Name and Address | |
| Ideal Research Inc.<br>11810 Parklawn Drive<br>Rockville, Maryland 20852 | 11. Contract or Grant No.<br>NAS3-22765 |
| | 13. Type of Report and Period Covered |
| 12. Sponsoring Agency Name and Address | Contractor Report |
| National Aeronautics and Space Administration<br>Washington, D.C. 20546 | 14. Sponsoring Agency Code<br>505-44-12 (E-1325) |

15. Supplementary Notes

Final report. Project Manager, Robert F. Ide, Propulsion Laboratory, AVRADCOM Research and Technology Laboratories, Lewis Research Center, Cleveland, Ohio.

16. Abstract

This report describes the development of an ice accretion measurement instrument that is a highly sensitive, accurate, rugged and reliable microprocessor controlled device using low level microwave energy for non-instrusive real time measurement and recording of ice growth history, including ice thickness and accretion rate. Data is displayed and recorded digitally. New experimental data is presented, obtained with the instrument, which demonstrates its ability to measure ice growth on a two-dimensional airfoil mounted in the NASA Lewis Research Center's Icing Research Tunnel. The device is suitable for aircraft icing protection. It may be mounted flush, non-intrusively, on any part of an aircraft skin including rotor blades and engine inlets.

| 17. Key Words (Suggested by Author(s)) | 18. Distribution Statement |
|---|---|
| Ice accretion; Microwave; Microprocessor; Non-intrusive; Real time; Digital display and recording; Aircraft | Unclassified - unlimited<br>STAR Category 06 |

| 19. Security Classif. (of this report) | 20. Security Classif. (of this page) | 21. No. of Pages | 22. Price* |
|---|---|---|---|
| Unclassified | Unclassified | 83 | A02 |

* For sale by the National Technical Information Service, Springfield, Virginia 22161

NASA-Langley, 1982